

## A fragment-based approach to targeting inosine-5'-monophosphate dehydrogenase (IMPDH) from *Mycobacterium tuberculosis*

Ana Trapero, Angela Pacitto, Vinayak Singh, Mohamad Sabbah, Anthony G Coyne, Valerie Mizrahi, Tom L. Blundell, David B. Ascher, and Chris Abell

*J. Med. Chem.*, **Just Accepted Manuscript** • DOI: 10.1021/acs.jmedchem.7b01622 • Publication Date (Web): 16 Mar 2018

Downloaded from <http://pubs.acs.org> on March 17, 2018

### Just Accepted

“Just Accepted” manuscripts have been peer-reviewed and accepted for publication. They are posted online prior to technical editing, formatting for publication and author proofing. The American Chemical Society provides “Just Accepted” as a service to the research community to expedite the dissemination of scientific material as soon as possible after acceptance. “Just Accepted” manuscripts appear in full in PDF format accompanied by an HTML abstract. “Just Accepted” manuscripts have been fully peer reviewed, but should not be considered the official version of record. They are citable by the Digital Object Identifier (DOI®). “Just Accepted” is an optional service offered to authors. Therefore, the “Just Accepted” Web site may not include all articles that will be published in the journal. After a manuscript is technically edited and formatted, it will be removed from the “Just Accepted” Web site and published as an ASAP article. Note that technical editing may introduce minor changes to the manuscript text and/or graphics which could affect content, and all legal disclaimers and ethical guidelines that apply to the journal pertain. ACS cannot be held responsible for errors or consequences arising from the use of information contained in these “Just Accepted” manuscripts.



1  
2  
3 A fragment-based approach to targeting inosine-5' -  
4  
5  
6 monophosphate dehydrogenase (IMPDH) from  
7  
8  
9 *Mycobacterium tuberculosis*  
10  
11  
12  
13

14 Ana Trapero,<sup>a</sup> Angela Pacitto,<sup>b</sup> Vinayak Singh,<sup>c#</sup> Mohamad Sabbah,<sup>a</sup> Anthony G. Coyne,<sup>a</sup>  
15 Valerie Mizrahi,<sup>c</sup> Tom L. Blundell,<sup>\*b</sup> David B. Ascher,<sup>\*b,d</sup> Chris Abell<sup>\*,a</sup>  
16  
17  
18  
19

20 <sup>a</sup> Department of Chemistry, University of Cambridge, Lensfield Road, Cambridge CB2 1EW,  
21 United Kingdom.  
22

23 <sup>b</sup> Department of Biochemistry, University of Cambridge, 80 Tennis Court Road, Cambridge  
24 CB2 1GA, United Kingdom.  
25  
26

27 <sup>c</sup> MRC/NHLS/UCT Molecular Mycobacteriology Research Unit & DST/NRF Centre of  
28 Excellence for Biomedical TB Research, Institute of Infectious Disease and Molecular Medicine  
29 and Division of Medical Microbiology, Faculty of Health Sciences, University of Cape Town,  
30 Rondebosch 7701, Cape Town, South Africa  
31  
32  
33  
34

35 <sup>d</sup> Department of Biochemistry and Molecular Biology, Bio21 Institute, University of Melbourne,  
36 30 Flemington Road, Parkville, Victoria 3052, Australia.  
37  
38

39 <sup>#</sup> Present address: H3D Drug Discovery and Development Centre, Department of Chemistry and  
40 Institute of Infectious Disease and Molecular Medicine, University of Cape Town, Rondebosch  
41 7701, Cape Town, South Africa  
42  
43  
44  
45  
46  
47  
48  
49

50 **ABSTRACT**

51 Tuberculosis (TB) remains a major cause of mortality worldwide, and improved treatments are  
52 needed to combat emergence of drug resistance. Inosine 5'-monophosphate dehydrogenase  
53 (IMPDH), a crucial enzyme required for *de novo* synthesis of guanine nucleotides, is an  
54  
55  
56  
57  
58  
59  
60

1  
2  
3 attractive TB drug target. Herein, we describe the identification of potent IMPDH inhibitors  
4 using fragment-based screening and structure-based design techniques. Screening of a fragment  
5 library for *Mycobacterium thermoresistibile* (*Mth*) IMPDH ( $\Delta$ CBS) inhibitors identified a low  
6 affinity phenylimidazole derivative. X-ray crystallography of the *Mth* IMPDH  $\Delta$ CBS  
7 –IMP–inhibitor complex revealed that two molecules of the fragment were bound in the NAD  
8 binding pocket of IMPDH. The linking the two molecules of the fragment afforded compounds  
9 with more than 1000-fold improvement in IMPDH affinity over the initial fragment hit.  
10  
11  
12  
13  
14  
15  
16  
17

18 **KEYWORDS:** IMPDH, *Mycobacterium tuberculosis*, fragment-based drug discovery, 2-  
19 acylaminoimidazole derivatives, X-ray crystallography.  
20  
21  
22  
23

## 24 INTRODUCTION

25 Tuberculosis (TB) is an contagious infectious disease caused by *Mycobacterium tuberculosis*  
26 (*Mtb*), which can be transmitted through the air as droplets. The infection predominantly affects  
27 the lungs, but can spread to other parts of the body, especially in patients with a suppressed  
28 immune system.  
29  
30  
31  
32  
33

34 The World Health Organization (WHO) has estimated that nearly one-third of the world's  
35 population is infected with *Mtb*, leading to 1.8 million TB deaths in 2015.<sup>1</sup> Although there has  
36 been a slow decline in new TB cases and TB-related deaths in recent years, the emergence and  
37 spread of multidrug resistant (MDR) and extensively drug resistant (XDR) strains of *Mtb* has  
38 increased the threat that this disease poses for global public health. According to the WHO  
39 approximately 480,000 cases of MDR-TB emerged in 2015, and the cure rate of those patients  
40 was only 50%.<sup>1</sup>  
41  
42  
43  
44  
45  
46  
47

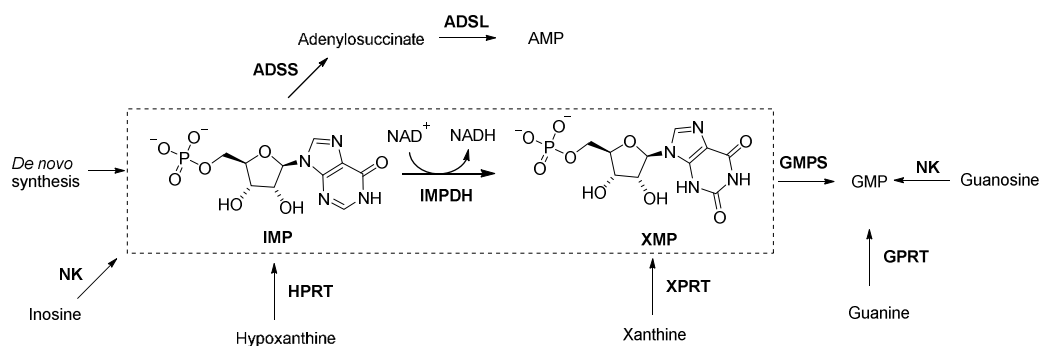
48 Current TB treatments require combinations of the four of the first-line drugs isoniazid,  
49 rifampicin, ethambutol, pyrazinamide and streptomycin, which must be taken for six months or  
50 longer.<sup>2</sup> Resistant strains are not susceptible to the standard drugs, and although MDR-TB is  
51 treatable using second-line drugs, such treatments have a number severe side effects.<sup>3</sup>  
52  
53  
54  
55  
56  
57  
58  
59  
60

Consequently, there is an urgent need for the development of novel and more effective drugs for the treatment of drug resistant TB.

Inosine-5'-monophosphate dehydrogenase (IMPDH, E.C. 1.1.1.205) has received considerable interest in recent years as an important target enzyme for immunosuppressive,<sup>4</sup> anticancer,<sup>5, 6</sup> and antiviral drugs.<sup>7</sup> Most recently, IMPDH has emerged as a promising antimicrobial drug target.<sup>8-11</sup>

IMPDH catalyzes the first unique step in the *de novo* synthesis of guanine nucleotides, the oxidation of inosine 5'-monophosphate (IMP) to xanthosine 5'-monophosphate (XMP) with the concomitant reduction of the cofactor nicotinamide adenine dinucleotide (NAD<sup>+</sup>) to NADH (Figure 1).<sup>12</sup> XMP is then subsequently converted to guanosine 5'-monophosphate (GMP) by a GMP synthetase.<sup>13</sup>

IMPDH has been deemed essential in every pathogen analyzed to date, including *Mtb*, *Staphylococcus aureus*, and *Pseudomonas aeruginosa*, which are three of the most serious bacterial threats.<sup>14-16</sup> However this has been somewhat contradictory,<sup>17</sup> in comparing cell versus animal work. IMPDH is an ubiquitous enzyme present in several eukaryotes, bacteria and protozoa.<sup>18</sup> The IMPDH reaction involves two chemical transformations. The first step of the IMPDH catalysed reaction involves the attack of catalytic Cys on substrate IMP followed by hydride transfer to NAD<sup>+</sup>, forming the covalent enzyme intermediate E-XMP\*. In the second step, E-XMP\* is hydrolysed to XMP.<sup>11</sup> The enzyme exists in two different conformations, an open form that accommodates both the substrate and cofactor during the first step, and a closed form where the active site flap moves into the NAD<sup>+</sup>-binding site for the E-XMP\* hydrolysis.<sup>19</sup>



1  
2  
3 **Figure 1.** Purine nucleotide biosynthesis. The commonly occurring guanine nucleotide  
4 biosynthetic and salvage reactions are shown, as is the adenine nucleotide biosynthetic pathway.  
5 The IMPDH reaction is boxed. NK, nucleoside kinase; HPRT, hypoxanthine phosphoribosyl  
6 transferase; XPRT, xanthine phosphoribosyl transferase; GPRT, guanine phosphoribosyl  
7 transferase; GMPS, guanosine 5'-monophosphate synthetase; GMPR, guanosine 5'-  
8 monophosphate reductase; ADSS, adenylosuccinate synthetase; ADSL, adenylosuccinate lyase.  
9  
10  
11  
12  
13  
14  
15

16  
17 In recent years, there has been considerable effort aimed at identifying small molecule inhibitors  
18 of IMPDH as potential antitubercular agents. X-ray crystal structures of a truncated form of the  
19 *Mtb* enzyme in complex with some of these compounds have been reported.<sup>20-26</sup>

20  
21 In antibacterial drug discovery, and especially in TB drug discovery, high-throughput screening  
22 (HTS) typically identifies a number of leads that show high potency *in vitro*, but most did not  
23 show any translation to an *in vivo* effect. It is also inevitable that the HTS libraries represent  
24 only a small fraction of possible chemical space and so limit confidence in finding a good  
25 starting point for subsequent development. Phenotypic screens can potentially lead to the  
26 identification of a molecule that modifies a disease phenotype by acting on a previously  
27 undescribed target or by acting simultaneously on more than one target.<sup>27</sup> However, for many of  
28 these hits the relevant target or targets has not yet been identified, thus preventing further target-  
29 based optimization of the compounds.<sup>28, 29</sup>

30  
31 The previously reported IMPDH inhibitors, such as compounds 7759844 (**1**), MAD1, P41,  
32 VCC234718 and DDD00079282 (Figure 2), were identified by phenotypic screening or target  
33 based HTS of compound libraries.<sup>21, 23-25</sup>

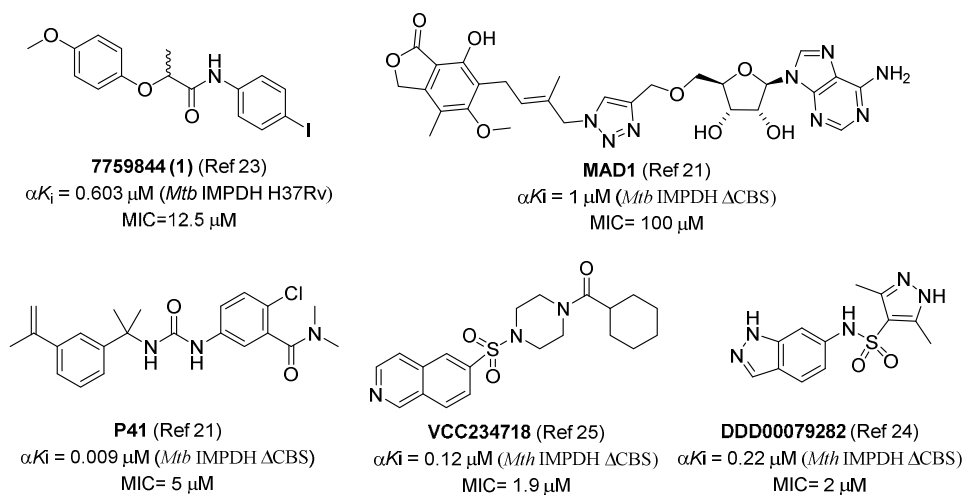
34  
35 We have sought to develop IMPDH inhibitors using a fragment-based approach. Fragment-  
36 based drug discovery (FBDD) is now established in both industry and academia as an  
37 alternative approach to high-throughput screening for the generation of hits or chemical tools  
38 for drug targets.<sup>30</sup>

39  
40 We have previously reported the discovery of several series of novel and potent inhibitors using  
41 FBDD to target *Mtb*. Previously we have reported the fragment elaboration strategies that we  
42  
43  
44  
45  
46  
47  
48  
49  
50  
51  
52  
53  
54  
55  
56  
57  
58  
59  
60

1  
2  
3 have applied which have included fragment growing, merging and linking. Although, fragment  
4 linking is conceptually the most appealing strategy for fragment elaboration, in practice, this  
5 strategy can be challenging where the choice of the optimal fragment linker can be crucial.<sup>31, 32</sup>

6  
7  
8 In the fragment-based approach, biophysical techniques are usually used to identify small  
9 chemical compounds (fragments) that bind with low affinity to the drug target. X-ray  
10 crystallography is then usually employed to establish the binding mode of the fragment and to  
11 facilitate the design of elaborated fragments. The availability of high-resolution X-ray crystal  
12 structures of a truncated form of the IMPDH,<sup>21, 24, 25</sup> in both the substrate-free and  
13 substrate/ligand-bound forms, make this enzyme attractive to a fragment-based approach.

14  
15  
16 In this work, the discovery of a new class of potent nM inhibitors of IMPDH using a FBDD  
17 approach is reported. A library of 960 fragments was screened against *Mth* IMPDH  $\Delta$ CBS using  
18 a biochemical assay. The fragment hits from this assay were examined using X-ray  
19 crystallography and an X-ray crystal structure of one of the fragment complexes was solved to a  
20 resolution of 1.45 Å. Examination of the X-ray crystal structure suggested a strategy of  
21 fragment-linking for optimization of this fragment hit.



49 **Figure 2.** Structures of previously reported IMPDH inhibitors ( $\alpha K_i$  values against IMP). All  
50 compounds showed uncompetitive inhibition with respect to IMP.  
51  
52  
53  
54  
55  
56  
57  
58  
59  
60

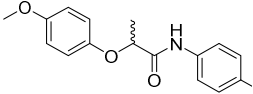
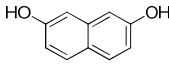
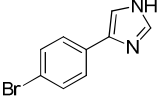
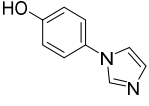
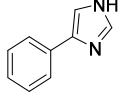
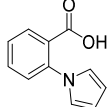
## RESULTS AND DISCUSSION

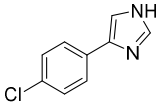
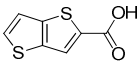
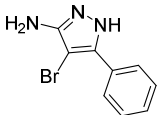
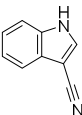
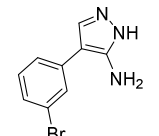
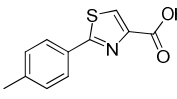
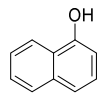
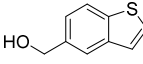
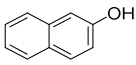
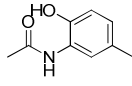
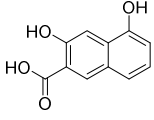
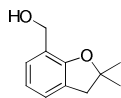
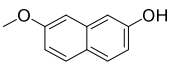
### Fragment Screening.

An in-house fragment library composed of 960 fragments was screened using a biochemical assay against *Mth* IMPDH  $\Delta$ CBS. *Mth* IMPDH, which shares 85% sequence identity with *Mtb* IMPDH and is 100% identical in the active site,<sup>24, 25</sup> was chosen for the fragment screening and structural studies because it gave higher protein expression yields and better diffracting crystals than the *Mtb* orthologue. IMPDH activity was monitored spectrophotometrically by measuring the formation of NADH at 340 nm. The biochemical assay was performed at a fragment concentration of 1 mM and hits were re-tested in triplicate. Compound **1** (7759844) previously reported as IMPDH inhibitor was used as a positive control in assays (Table 1).<sup>23</sup>

The screen resulted in 18 hits (1.9% hit rate), where a hit was defined as a compound that gave greater than 50% inhibition at a concentration of 1 mM. A complete list of fragments hits identified is included in Table 1. A number of common scaffolds were observed, in particular phenylimidazole (fragments **2–4**), aminopyrazole (fragments **5–6**) and naphthol (fragments **7–11**), and the remaining compounds contained a substituted phenyl or a heterocyclic five membered ring (fragments **12–19**).

**Table 1. Structures and activities for compound 1 (7759844) and the most potent fragment hits found in the screen against *Mth* IMPDH  $\Delta$ CBS**

Compd	Structure	% Inhibition at 1 mM	Compd	Structure	% Inhibition at 1 mM
<b>1</b>		92 ± 1 <sup>a</sup>	<b>11</b>		77 ± 1
<b>2</b>		65 ± 2	<b>12</b>		64 ± 6
<b>3</b>		52 ± 4	<b>13</b>		72 ± 1

4		59 ± 1	14		86 ± 6
5		53 ± 3	15		51 ± 1
6		50 ± 3	16		88 ± 10
7		68 ± 3	17		53 ± 2
8		57 ± 1	18		79 ± 4
9		98 ± 2	19		99 ± 1
10		66 ± 1			

<sup>a</sup>% Inhibition at 10 μM.

The IC<sub>50</sub> values of six of the most active fragments were measured and the IC<sub>50</sub> and ligand efficiency (LE) values of these fragments are summarized in Table 2. The fragment screen provided an array of hits with IC<sub>50</sub> ranging from 325 μM to 674 μM and ligand efficiencies from 0.31 to 0.42. The inhibition constant [*K*<sub>i</sub>] with respect to both substrates IMP and NAD<sup>+</sup> were determined by assaying various concentrations of each inhibitor with five different concentrations of substrate and a fixed saturating concentration of the co-substrate. The inhibition data for these fragments are summarized in Table 2. All compounds yielded an uncompetitive inhibition pattern with respect to NAD<sup>+</sup> with *K*<sub>i</sub> values ranging from 262 to 525 μM. Fragments **14**, **16** and **19** yielded a mixed inhibition with respect to IMP with *K*<sub>i</sub> values ranging from 126 to 398 μM and compounds **1**, **2**, **11** and **18** yielded an uncompetitive inhibition with *K*<sub>i</sub> values ranging from 361 to 609 μM.

Inhibition constants of compound **2** towards full-length *Mtb* IMPDH were also determined.

Compound **2** inhibited full-length *Mtb* IMPDH enzyme with a *K*<sub>i</sub> value of 572 ± 14 μM with

IMP as the substrate and a  $K_i$  value of  $534 \pm 18 \mu\text{M}$  with NAD as the substrate, which are similar to the  $K_i$  values observed for the *Mth* IMPDH  $\Delta\text{CBS}$  enzyme.

**Table 2. IC<sub>50</sub>, Ligand Efficiency, and alpha  $K_i$  values of fragment hits and compound 1 (7759844) against *Mth* IMPDH  $\Delta\text{CBS}$**

Compd	IC <sub>50</sub> ( $\mu\text{M}$ ) (LE) <sup>a</sup>	IMP $\alpha K_i$ ( $\mu\text{M}$ )	NAD $\alpha K_i$ ( $\mu\text{M}$ )
<b>1</b>	$0.77 \pm 0.06$ (0.40)	$0.86 \pm 0.03$ (UC) <sup>b</sup>	$0.55 \pm 0.02$ (UC)
<b>2</b>	$674 \pm 53$ (0.36)	$609 \pm 3$ (UC)	$512 \pm 23$ (UC)
<b>11</b>	$336 \pm 6$ (0.39)	$361 \pm 53$ (UC)	$310 \pm 30$ (UC)
<b>14</b>	$400 \pm 7$ (0.42)	$238 \pm 6$ (Mixed)	$262 \pm 39$ (UC)
<b>16</b>	$433 \pm 60$ (0.31)	$398 \pm 81$ (Mixed)	$525 \pm 64$ (UC)
<b>18</b>	$512 \pm 37$ (0.37)	$554 \pm 70$ (UC)	$452 \pm 26$ (UC)
<b>19</b>	$325 \pm 9$ (0.37)	$126 \pm 34$ (Mixed)	$355 \pm 47$ (UC)

<sup>a</sup>Ligand efficiency was calculated using the equation  $\text{LE} = (1.37 \times \text{pIC}_{50})/\text{HA}$ , where HA means heavy atom, i.e., a non-hydrogen atom. <sup>b</sup>UC: Uncompetitive inhibition.

### X-ray Structure of compounds 1 (7759844) and 2

Compound **1** and the six fragment hits (**2**, **11**, **14**, **16**, **18** and **19**) were selected for structural characterization using X-ray crystallography by soaking into preformed crystals of *Mth* IMPDH  $\Delta\text{CBS}$  as previously described.<sup>20</sup> After molecular replacement, clear electron density was observed in the  $2F_0 - F_c$  difference map ( $\sigma = 3.0$ ) for IMP, and in addition density was observed for one molecule of compound **1** (Figure 3A) and two molecules of compound **2** (Figure 3B), which were partially occupying the  $\text{NAD}^+$  binding site. None of the other fragments (**11**, **14**, **16**, **18** and **19**) showed any electron density in the X-ray crystal structures. Although the kinetic

1  
2  
3 studies of compounds **1** and **2** suggested that these two compounds are uncompetitive with  
4 respect to NAD<sup>+</sup>, the binding mode of compounds **1** and **2** closely resemble that of other  
5 previously reported uncompetitive inhibitors of *Mtb* IMPDH.<sup>21, 24, 25</sup> It has been proposed that  
6 the uncompetitive mode of inhibition of IMPDH inhibitors with respect to NAD<sup>+</sup> is consistent  
7 with their binding preferentially to the covalent IMPDH-XMP\* intermediate after NADH has  
8 been released.<sup>24, 25, 33</sup>

9  
10  
11 The structure of *Mth* IMPDH ΔCBS with compound **1** showed that the inhibitor binds in the  
12 NAD pocket in a near identical manner to our recently described IMPDH inhibitors.<sup>24, 25</sup>

13  
14  
15  
16  
17  
18  
19  
20  
21  
22  
23  
24  
25  
26  
27  
28  
29  
30  
31  
32  
33  
34  
35  
36  
37  
38  
39  
40  
41  
42  
43  
44  
45  
46  
47  
48  
49  
50  
51  
52  
53  
54  
55  
56  
57  
58  
59  
60  
Compound **1** formed strong  $\pi$  interactions with the hypoxanthine group of IMP, P45', Y471',  
and polar interactions with G409, E442, P45' and G470'. The electron density revealed two  
molecules of compound **2** within the NAD binding pocket of IMPDH. One molecule of  
compound **2** stacked with IMP, forming extensive  $\pi$  interactions with the hypoxanthine group of  
IMP. This fragment was further stabilised through polar interactions, hydrogen bonds and  $\pi$   
interactions to surrounding residues in the active site pocket, including A269, G318 and E442.  
The other molecule of compound **2** sits closer to the opening of the active site, making polar  
interactions with N273 and E442, and  $\pi$  interactions with H270 and Y471'.

A comparison of the structure of *Mth* IMPDH ΔCBS with compound **1** with the fragment **2**  
structure shows that the two molecules of **2** mimic the position of the larger inhibitor **1** (Figure  
3C).

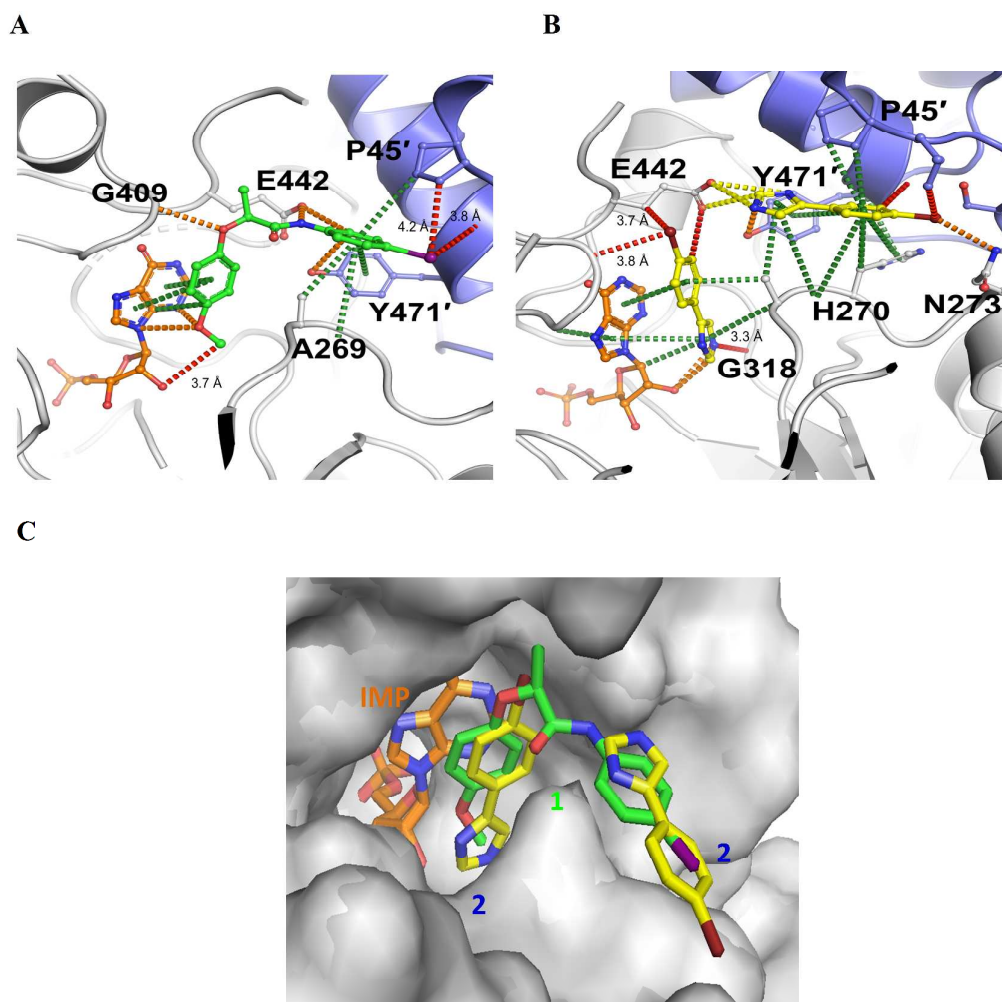


**Figure 3.** X-ray crystal structure of compounds **1** and **2** bound to IMPDH. Ligand interactions are represented as dotted lines; hydrogen bonds are represented in red, polar interactions in orange, ionic interactions in yellow and aromatic and  $\pi$  interactions in green dotted lines. Protein–ligand interactions were analyzed using Arpeggio. (a) Interactions made by **1** (green) in the X-ray crystal structure of the complex of IMPDH with IMP (orange). (b) Interactions made by **2** (yellow) in the X-ray crystal structure of the complex of IMPDH with IMP. (c) Structural alignment of the IMPDH crystal structures of **1** (green) and **2** (yellow).

### Fragment elaboration

Fragment **2** was selected as the starting point for exploration because of the ease of synthetic modification and the availability of a X-ray crystal structure to guide the optimization. For

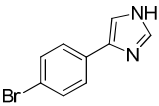
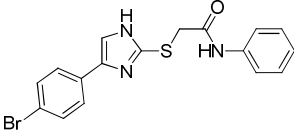
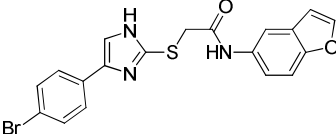
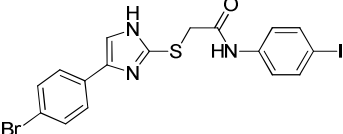
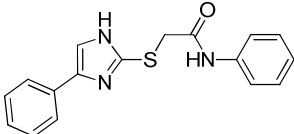
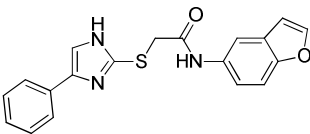
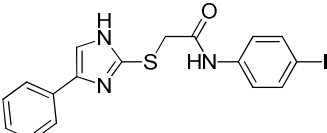
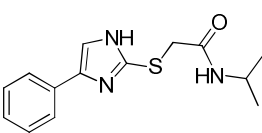
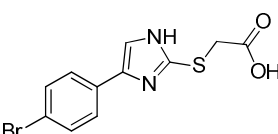
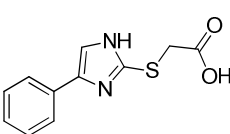
1  
2  
3 chemical elaboration of **2**, fragment linking as well as fragment growing were considered. As  
4 the two molecules of fragment **2** are found to bind in adjacent regions of the target protein, the  
5 fragment-linking approach was the more attractive option. However, before fragment linking,  
6 fragment **2** was further optimised with the aim of improving the binding affinity. The structures  
7 and inhibitory activities of these compounds against *Mth* IMPDH  $\Delta$ CBS are summarized in  
8 Tables 3 and 4. The corresponding data for fragment **2** have also been included for comparative  
9 purposes.

10  
11 All compounds were evaluated at a concentration of 100  $\mu$ M with *Mth* IMPDH  $\Delta$ CBS.

### 12 13 14 15 16 17 18 19 20 21 **Fragment growing.**

22 The fragment-growing strategy involves using structure-based drug design to form additional  
23 interactions by growing out from the starting fragment. Fragment **2** was modified at the 2-  
24 position of the imidazole ring to explore the introduction of various aromatic rings linked by a  
25 thioacetamide (**20–22**) to form  $\pi$  interactions with the hypoxanthine group of IMP (Figure S1).  
26 Such modifications gave compounds with improved *Mth* IMPDH  $\Delta$ CBS inhibition. The phenyl  
27 and benzofuran derivatives (**20** and **21**), showed 13 and 31% inhibition, respectively. *Mth*  
28 IMPDH  $\Delta$ CBS inhibition was shown to be sensitive to minor modifications of the phenyl  
29 substituent groups e.g. the 4-iodo substituted **22** showed 30% inhibition at 100  $\mu$ M, whereas the  
30 non-substituted compound, **20**, showed 13% inhibition at the same concentration. The effect of  
31 the removal of the 4-bromo group was investigated and compounds **23–25** were synthesized.  
32 Removal of the bromo substituent in compounds **20–22** (13–31% inhibition at 100  $\mu$ M) was  
33 tolerated (**23–25**, 3–46% inhibition at 100  $\mu$ M). The importance of the aromatic amide linked  
34 by a thioacetamide was subsequently examined. Replacing the phenyl with isopropyl (**26**)  
35 resulted in complete loss of activity. Substitution of the thioacetamide by a thioacetic acid also  
36 led to a complete loss in activity (compounds **27** and **28**).  
37  
38  
39  
40  
41  
42  
43  
44  
45  
46  
47  
48  
49  
50  
51  
52  
53  
54  
55  
56  
57  
58  
59  
60

Table 3. Structures and activities for fragment 2 and compounds 20–28 against *Mth*IMPDH  $\Delta$ CBS

Compd	Structure	% Inhibition at 100 $\mu$ M
2		< 5%
20		13 $\pm$ 3
21		31 $\pm$ 6
22		30 $\pm$ 3
23		< 5%
24		36 $\pm$ 1
25		46 $\pm$ 3
26		< 5%
27		< 5%
28		< 5%

### Fragment linking and SAR.

Examination of the X-ray crystal structure of the previously reported inhibitor **1** when overlaid with fragment **2** revealed that the distance between the 4-position of the phenyl ring of fragment **2** and the 2-position of the imidazole ring represents the closest approach of the molecules (Figure S1). On the basis of this structural information, three different linkers were designed to connect the two copies of the fragment **2** at these positions (compounds **29–31**). Initially, a thioacetamide and urea linker moieties were examined. Compounds **29** and **30** showed 20% and 56% of *Mth* IMPDH  $\Delta$ CBS inhibition respectively, at 100  $\mu$ M (Table 4). Interestingly, compound **30** showed a 12-fold improvement in *Mth* IMPDH  $\Delta$ CBS inhibitory activity with an  $IC_{50}$  of 58  $\mu$ M, compared to the fragment **2**.

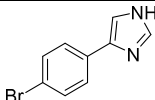
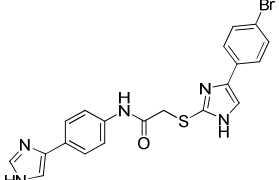
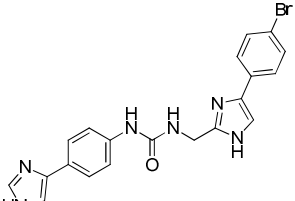
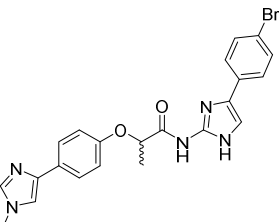
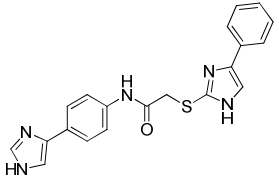
The lactate linker was then used but all attempts to link 4-phenylimidazole with 4-(4-bromophenyl)-1*H*-imidazole were unsuccessful. We therefore decided to synthesize compound **31**, which contains 1-methyl-4-phenyl-1*H*-imidazole and 4-(4-bromophenyl)-1*H*-imidazole linked with a lactate analogue, as in compound **1**. Compound **31** (Table 4) showed markedly improved *Mth* IMPDH  $\Delta$ CBS inhibition with a LE of 0.29 and  $IC_{50}$  of 0.52  $\mu$ M, which is 1300-fold more potent compared to the fragment **2**. Although compound **31** binds in the cofactor site, the mechanism of inhibition can vary depending on its relative affinities for the E•IMP and E-XMP\* complexes.<sup>8, 11</sup> Kinetic evaluation of compound **31** showed the mode of *Mth* IMPDH  $\Delta$ CBS inhibition was uncompetitive with respect to both IMP and the  $NAD^+$  cofactor (see Figure S2, Supporting Information) with a  $K_i$  value of  $0.30 \pm 0.02$   $\mu$ M with IMP as the substrate and a  $K_i$  value of  $0.20 \pm 0.01$  with NAD as the substrate.

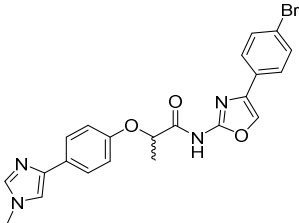
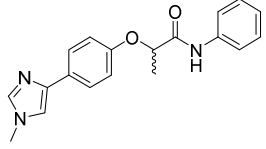
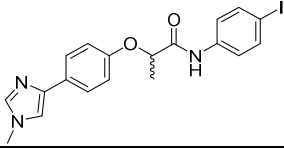
Inhibition constants of compound **31** towards full-length *Mtb* IMPDH were also determined. Compound **31** inhibited full-length *Mtb* IMPDH enzyme with a  $K_i$  value of  $0.61 \pm 0.05$   $\mu$ M with IMP as the substrate and a  $K_i$  value of  $0.39 \pm 0.02$   $\mu$ M with NAD as the substrate. The inhibition constants were consistent with the data using the *Mth* IMPDH  $\Delta$ CBS enzyme.

Removal of the bromo substituent in compound **29** to give compound **32** was well tolerated (Table 4). The importance of the imidazole group for the inhibitory activity against *Mth* IMPDH  $\Delta$ CBS was confirmed by replacing of the 4-(4-bromophenyl)-1*H*-imidazole substituent of

compound **31** with 4-(4-bromophenyl)oxazole (**33**) which resulted in a 4-fold loss of activity (Table 4). Replacing the 4-(4-bromophenyl)-1*H*-imidazole of **31** by a phenyl (**34**) resulted in complete loss of activity (Table 4). However, the 4-iodophenyl derivative **35** demonstrated slightly improved activity ( $IC_{50} = 0.47 \mu\text{M}$ ,  $LE = 0.34$ ) compared to compounds **31** ( $IC_{50} = 0.52 \mu\text{M}$ ,  $LE = 0.29$ ) and **1** ( $IC_{50} = 0.77 \mu\text{M}$ ,  $LE = 0.40$ ). It is noteworthy that  $LE$  of compound **35** was comparable to that of the original fragment hit **2** ( $LE=0.36$ ) and other reported IMPDH inhibitors.<sup>34</sup>

**Table 4. Structures and activities for fragment 2 and compounds 29–35 against *Mth* IMPDH  $\Delta$ CBS**

Compd	Structure	% Inhibition at 100 $\mu\text{M}$	$IC_{50}$ ( $\mu\text{M}$ ) ( $LE$ ) <sup>a</sup>
<b>2</b>		< 5%	$674 \pm 53$ (0.36)
<b>29</b>		$20 \pm 5$	ND <sup>b</sup>
<b>30</b>		$56 \pm 11$	$58 \pm 8$ (0.21)
<b>31</b>		$99 \pm 11$ <sup>c</sup>	$0.52 \pm 0.004$ (0.29)
<b>32</b>		$24 \pm 1$	ND

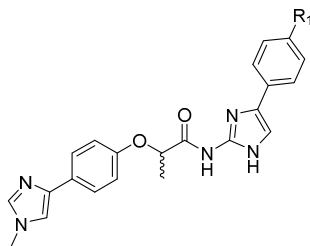
1			
2			
3			
4			
5			
6	<b>33</b>		$83 \pm 2^c$ $2.21 \pm 0.08$ (0.26)
7			
8			
9			
10			
11	<b>34</b>		$4 \pm 1^c$ ND
12			
13			
14			
15	<b>35</b>		$97 \pm 1^c$ $0.47 \pm 0.03$ (0.34)
16			
17			
18			
19			

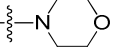
<sup>a</sup>Ligand efficiency was calculated using the equation  $LE = (1.37 \times pIC_{50})/HA$ , where HA means heavy atom, i.e., a non-hydrogen atom. <sup>b</sup>ND: not determined.  $IC_{50}$  values were determined for compounds that showed >50% inhibition. <sup>c</sup>%Inhibition at 10  $\mu$ M.

The importance of the 4-bromo substituent on phenyl ring in compound **31** was also explored (compounds **36–39**, Table 5). Removal of the bromo substituent (**36**) resulted in a 5-fold loss in activity. Whereas replacing this group with an iodine (**39**) or a morpholine ring (**37**) resulted in less than 1.3-fold loss in activity. The electronic nature of the substituent in this position had little effect on inhibitory activity. For example, an electron-donating methoxy (**38**) retained activity comparable to the bromine derivative (**31**). Among them, imidazoles **31**, **37–38**, and **39** were found to be potent inhibitors of *Mth* IMPDH  $\Delta$ CBS with  $IC_{50}$  values ranging from 520 to 690 nM.

The (*S*)-isomer of **31** was found to bind preferentially (Table 5), the racemate **31** having approximately half the *Mth* IMPDH  $\Delta$ CBS inhibition of the (*S*)-isomer **31**. This observation accords with the results previously reported for other series of IMPDH inhibitors.<sup>21,35</sup>

**Table 5. Structures and activities for compounds 31, 36–39, and (S)-31 against *Mth* IMPDH ΔCBS**

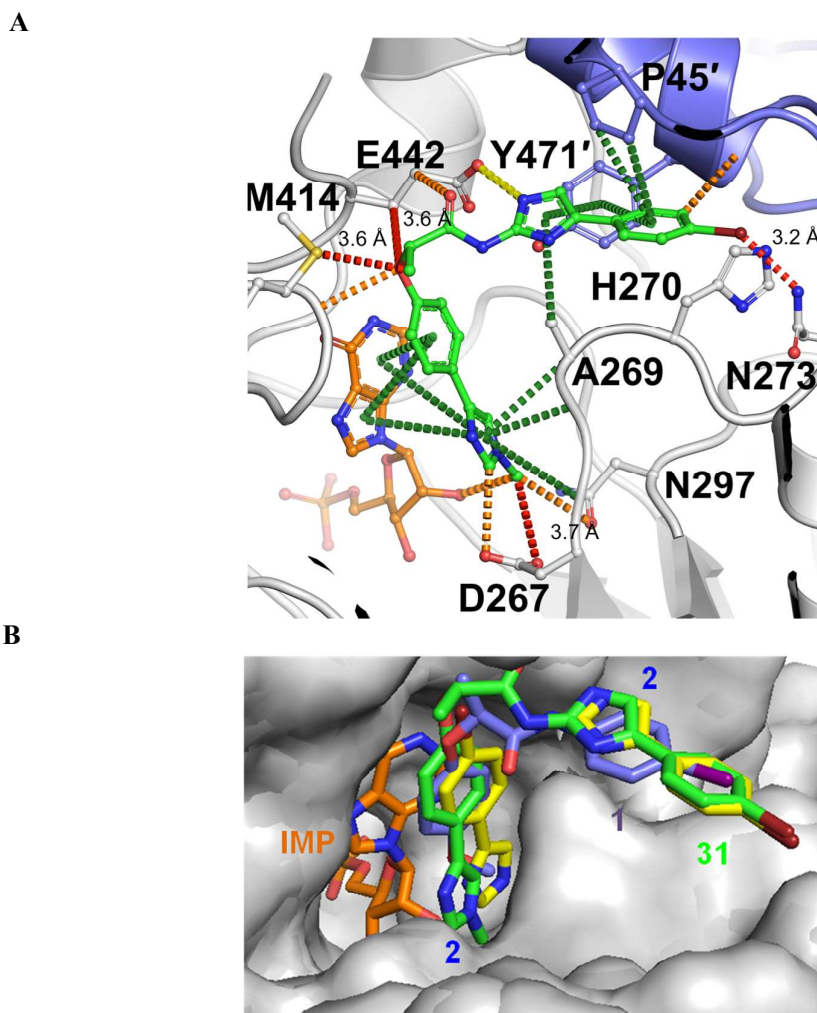


Compd	R <sub>1</sub>	% Inhibition at 10 μM	IC <sub>50</sub> (μM) (LE) <sup>a</sup>
<b>31</b>	Br	99 ± 1	0.52 ± 0.004 (0.29)
<b>36</b>	H	77 ± 3	2.76 ± 0.21 (0.26)
<b>37</b>		94 ± 1	0.52 ± 0.01 (0.24)
<b>38</b>	OMe	95 ± 1	0.64 ± 0.03 (0.27)
<b>39</b>	I	96 ± 1	0.69 ± 0.06 (0.28)
<b>(S)-31</b>	Br	99 ± 1	0.27 ± 0.02 (0.30)

<sup>a</sup>Ligand efficiency was calculated using the equation  $LE = (1.37 \times pIC_{50})/HA$ , where HA means heavy atom, i.e., a non-hydrogen atom.

### X-ray structure of compound 31

From crystals soaked with compound **31**, the  $2F_0 - F_c$  difference map ( $\sigma = 3.0$ ) revealed strong density for the inhibitor. The structure of compound **31** (Figure 4A) showed that it bound in a nearly identical manner to compounds **1** and **2** in the NAD binding pocket (Figure 4B), stacking with IMP, and maintaining the interactions with H270, N273, E442, and P45 and Y471 from the neighbouring subunit. Compound **31** made additional interactions in the binding pocket, including polar interactions with D267 and N297.



36  
37  
38  
39  
40  
41  
42  
43  
44  
45  
46  
47  
48  
49

**Figure 4.** X-ray crystal structure of compound **31** bound to IMPDH. Protein–ligand interactions were analyzed using Arpeggio. (a) Interactions made by **31** in the X-ray crystal structure of the complex of IMPDH with IMP (orange). Ligand interactions are represented as dotted lines; hydrogen bonds are represented in red, polar interactions in orange, ionic interactions in yellow and aromatic and  $\pi$  interactions in green dotted lines. (b) Structural alignment of the IMPDH crystal structures of **1** (lilac), **2** (yellow) and **31** (green).

50  
51

#### Whole-cell activity against *Mtb*.

52  
53  
54  
55  
56  
57  
58  
59  
60

The whole-cell activity of the most potent analogues **31**, **33–39**, and (*S*)-**31** *in vitro* was determined against *Mtb* H37Rv (see Table S1, Supporting Information). No significant inhibition of bacterial growth was detected for any of the compounds ( $\text{MIC}_{90} \geq 50 \mu\text{M}$ ) over the

1  
2  
3 tested concentration range (0–100  $\mu$ M). There are currently on-going efforts to explain the lack  
4 of efficacy of the potent *Mth* IMPDH  $\Delta$ CBS inhibitors described which could be caused by low  
5 membrane permeability, poor metabolic stability and/or drug-efflux mechanisms.  
6  
7  
8  
9

### 10 11 **Synthetic Chemistry.**

12  
13 Compounds **20–29** and **32** were synthesized from 4-phenyl-1*H*-imidazole-2-thiol or 4-(4-  
14 bromophenyl)-1*H*-imidazole-2-thiol according to the sequence described in Scheme 1.  
15 Thioacetic derivatives **27** and **28** were prepared by treatment of 4-phenyl-1*H*-imidazole-2-thiol  
16 or 4-(4-bromophenyl)-1*H*-imidazole-2-thiol with 2-chloroacetic acid in the presence of NaOH  
17 followed by neutralization with hydrochloric acid.  
18  
19  
20  
21

22  
23 Thioacetamide **26** was synthesized by amide coupling between thioacetic derivative **28** and  
24 isopropylamine. Similarly, thioacetamides **20–25**, **29** and **32** were prepared by cross-linking 4-  
25 phenyl-1*H*-imidazole-2-thiol or 4-(4-bromophenyl)-1*H*-imidazole-2-thiol with  $\alpha$ -  
26 chloroacetamides **40–43**, which were obtained by acylation of anilines with various substituents  
27 with chloroacetyl chloride.  
28  
29  
30  
31

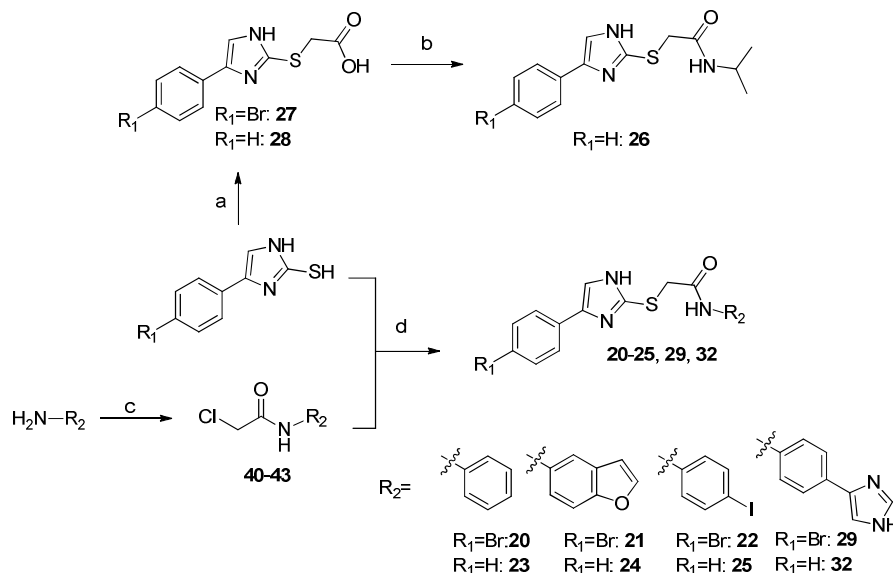
32  
33 The synthesis of urea **30** was achieved as shown in Scheme 2 by coupling amine **44** and *N*-(4-  
34 (1*H*-imidazol-4-yl)phenyl)-1*H*-imidazole-1-carboxamide, which was obtained from  
35 commercially available 4-(1*H*-imidazol-4-yl)aniline as a crude intermediated, in the presence of  
36 *N,N*-diisopropylethylamine. Amine **44** was synthesized from benzyl ((5-(4-bromophenyl)-1*H*-  
37 imidazol-2-yl)methyl)carbamate,<sup>36</sup> followed by the deprotection of the benzyloxycarbonyl  
38 group under acidic condition.  
39  
40  
41  
42  
43

44  
45 Imidazole derivatives **31**, **36–38**, and **39** were prepared following the synthetic procedure  
46 outlined in Scheme 3. 2-Aminoimidazoles **50–54** were synthesized according to a published  
47 microwave-assisted protocol.<sup>37</sup> In brief, 2-aminoimidazoles **50–54** were prepared by reaction of  
48 the commercially available  $\alpha$ -haloketones and *N*-acetylguanidine, followed by deacetylation  
49 (Scheme 3). Acid **59** was synthesized starting with imidazole **55**, which was prepared by  
50 reaction of 2-bromo-4'-hydroxyacetophenone with formamide as reported previously.<sup>38</sup> The  
51 phenol **57** was synthesized by alkylation of imidazole **55**, followed by deprotection of the  
52  
53  
54  
55  
56  
57  
58  
59  
60

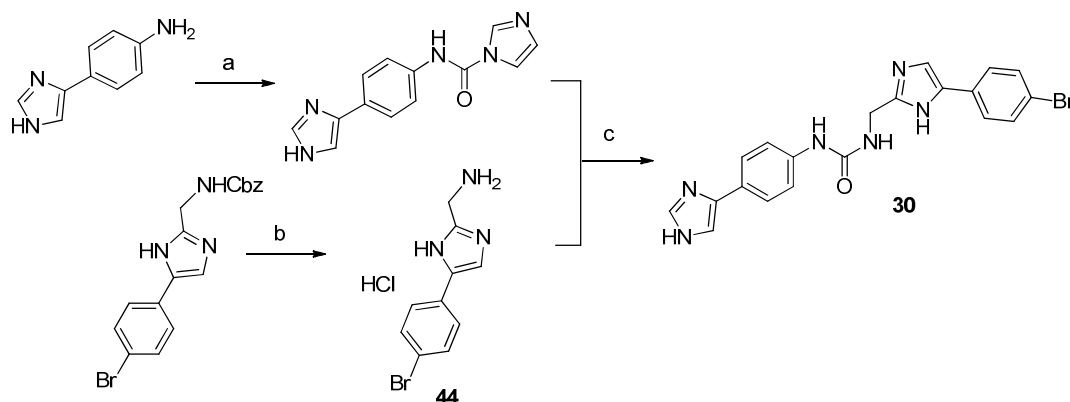
1  
2  
3 methyl ether with  $\text{BBr}_3$ . Substituted phenol **57** was converted to the ether **58** upon treatment  
4  
5 with methyl 2-bromopropionate in the presence of  $\text{Cs}_2\text{CO}_3$ . Enantiomerically pure phenyl ethers  
6  
7 were synthesized by using Mitsunobu reaction conditions with ethyl D-lactate (Scheme 4). After  
8  
9 the hydrolysis of the ester group, the resulting carboxylic acid **59** was treated with thionyl  
10  
11 chloride to give the acid chloride **60**, which was reacted with 2-aminoimidazoles **50–54** to  
12  
13 afford imidazole derivatives **31**, **36–38**, and **39**.

14  
15 The synthesis of 2-acylaminooxazole **33** and amides **34–35** were achieved as shown in Scheme  
16  
17 5. 2-acylaminooxazole derivative **33** was obtained by coupling the acid chloride derivative **60**  
18  
19 with 2-aminooxazole derivative **61**, which was prepared by reaction of 2,4'-  
20  
21 dibromoacetophenone with urea. Similarly, amides **34–35** were prepared by coupling the  
22  
23 corresponding anilines with the acid chloride derivative **60**.

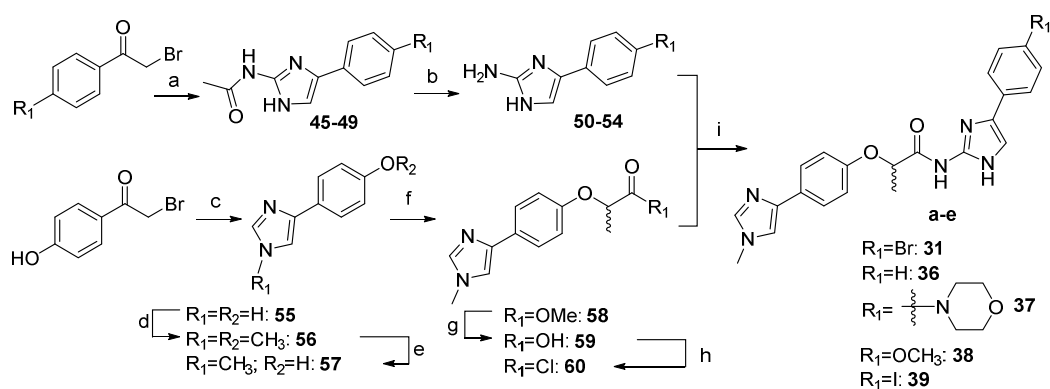
24  
25  
26 **Scheme 1. Synthesis of thioacetamide and thioacetic derivatives 20–29 and 32<sup>a</sup>**



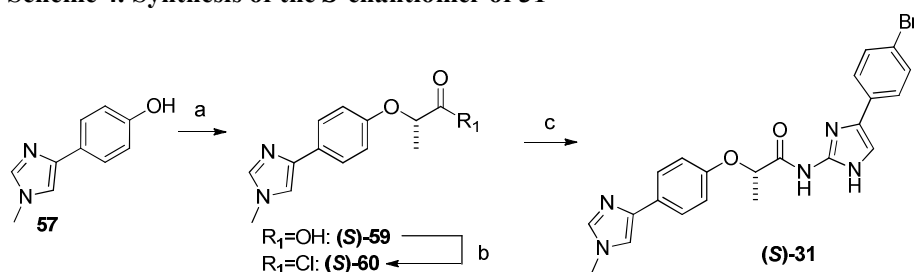
<sup>a</sup> Reagent and conditions: (a) 2-chloroacetic acid, NaOH, EtOH, 80 °C, 69–72%; (b) isopropylamine, HATU, DIPEA, EtOAc, rt, 73%; (c) chloroacetyl chloride, TEA, DCM, rt, 89–99%; (d) NaOH, MeOH, H<sub>2</sub>O, 70 °C, 69–96%.

Scheme 2. Synthesis of urea 30<sup>a</sup>

<sup>a</sup> Reagent and conditions: (a) CDI, THF, rt, quant.; (b) HCl (4M), dioxane, 100 °C, quant.; (c) DIPEA, DMF, rt, 26%.

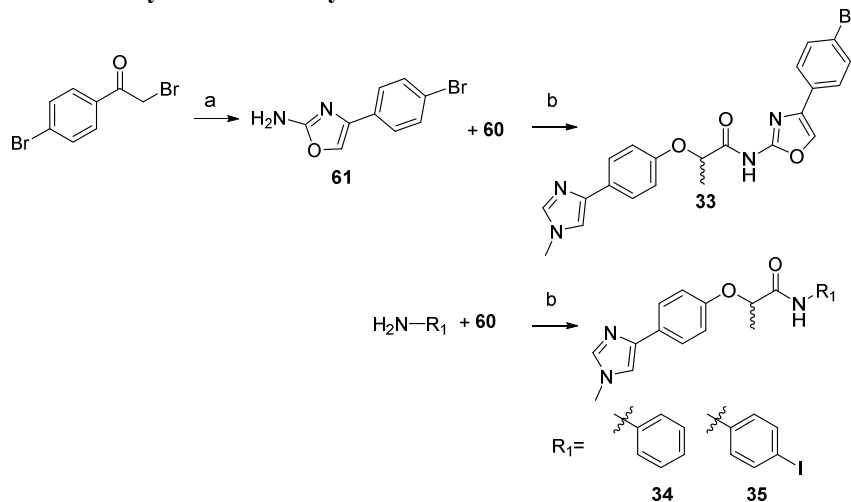
Scheme 3. Synthesis of 2-acylaminoimidazole derivatives 31, 36–38, and 39<sup>a</sup>

<sup>a</sup> Reagent and conditions: (a) acetylguanidine, CH<sub>3</sub>CN,  $\mu$ W, 100 °C, 71–88%; (b) 1. 20% H<sub>2</sub>SO<sub>4</sub>, MeOH:H<sub>2</sub>O (1:1 v/v),  $\mu$ W, 100 °C; 2. aq. Na<sub>2</sub>CO<sub>3</sub>, 79–95%; (c) formamide, 150 °C, 99%; (d) CH<sub>3</sub>I, Cs<sub>2</sub>CO<sub>3</sub>, DMF, rt, 88%; (e) BBr<sub>3</sub> (1M in DCM), -78°C–rt, DCM, 96%; (f) Cs<sub>2</sub>CO<sub>3</sub>, methyl 2-bromopropionate, DMF, 60 °C, 92%; (g) NaOH, THF:H<sub>2</sub>O (2:1 v/v), 80 °C, 65%; (h) SOCl<sub>2</sub>, 80 °C, quant.; (i) TEA, DCM, 40 °C, 61–72%.

Scheme 4. Synthesis of the *S*-enantiomer of 31<sup>a</sup>

<sup>a</sup> Reagent and conditions: (a) 1. Ethyl D-lactate, PPh<sub>3</sub>, DEAD, THF, rt; 2. NaOH, THF:H<sub>2</sub>O (2:1 v/v), rt, 56%; (b) SOCl<sub>2</sub>, 80 °C, quant.; (c) 50, TEA, DCM, 40 °C, 69%.

**Scheme 5. Synthesis of 2-acylaminooxazole derivative **33** and amides **34–35**<sup>a</sup>**



<sup>a</sup>Reagent and conditions: (a) urea,  $\text{CH}_3\text{CN}$ , 80 °C, 78%; (b) TEA, DCM, rt (for **34** and **35**) or 40 °C (for **33**), 64–76%.

## CONCLUSIONS

FBDD has emerged as a robust approach to identify small molecules that bind to a wide range of therapeutic targets. Fragment elaboration strategies have resulted in the development of a number of compounds that have progressed into clinical trials. Within the area of TB drug discovery, a number of HTS and phenotypic screens have been performed during the past decade. Although HTS identified a number of leads that show high potency *in vitro*, the translation to an *in vivo* effect has proven challenging.

This study illustrates the successful application of a fragment-based approach followed by fragment optimization to obtain nanomolar affinity ligands of IMPDH. A library of 960 fragments were screened against *Mth* IMPDH  $\Delta\text{CBS}$ , and from the screen the phenylimidazole fragment hit **2** ( $\text{IC}_{50} = 674 \mu\text{M}$ ) was identified. Kinetic experiments showed that **2** was an uncompetitive inhibitor of *Mth* IMPDH  $\Delta\text{CBS}$  with respect to  $\text{NAD}^+$  and IMP. Two molecules of the fragment **2** were shown to bind at the NAD binding site of the enzyme. The X-ray crystal structure also revealed that one molecule of fragment **2** makes  $\pi$  interactions with IMP and the other molecule sits closer to the opening of the active site, making polar interactions with N273 and E442, and  $\pi$  interactions with H270 and Y471'. This provides potential for further

1  
2  
3 optimization of fragment **2**. To explore better the possibilities given by fragment **2**, fragment-  
4 linking and fragment-growing strategies were employed, resulting in low micromolar to  
5 nanomolar affinity compounds. Among them, compounds **31**, **35**, **37–39** were the most potent  
6  
7  
8  
9  
10  
11  
12  
13  
14  
15  
16  
17  
18  
19  
20  
21  
22  
23  
24  
25  
26  
27  
28  
29  
30  
31  
32  
33  
34  
35  
36  
37  
38  
39  
40  
41  
42  
43  
44  
45  
46  
47  
48  
49  
50  
51  
52  
53  
54  
55  
56  
57  
58  
59  
60

IMDPH inhibitors of the series described in this work with  $IC_{50}$  values between 0.47 and 0.69  $\mu$ M, which represent >1000-fold improvement in *Mth* IMPDH  $\Delta$ CBS potency over the initial fragment hit. Compound **31** was shown to bind at the NAD binding site of the enzyme and the X-ray crystal structure also revealed that it makes  $\pi$  interactions with IMP, and maintaining the interactions with H270, N273, E442, and P45 and Y471 from the neighbouring subunit. Moreover, compound **31** made additional interactions in the binding pocket, including polar interactions with D267 and N297. A comparison of this structure with the fragment **2** structure shows that the two molecules of **2** mimic the position of the larger inhibitor **31**. This is the first example of utilizing the fragment-based approach specifically to identify new potent inhibitors of IMPDH. Further structural optimization to improve the cellular activity of these analogues is ongoing with the aim of developing novel classes of anti-TB agents.

## EXPERIMENTAL SECTION

### 1. Chemistry

**1.1 General Experimental Methods.** Solvents were distilled prior to use and dried by standard methods. Unless otherwise stated,  $^1\text{H}$  and  $^{13}\text{C}$  NMR spectra were obtained in  $\text{CDCl}_3$ , MeOD, or  $\text{DMSO}-d_6$  solutions using either a Bruker 400 MHz AVANCE III HD Smart Probe, 400 MHz QNP cryoprobe, or 500 MHz DCH cryoprobe spectrometer. Chemical shifts ( $\delta$ ) are given in ppm relative to the residual solvent peak ( $\text{CDCl}_3$ :  $^1\text{H}$ ,  $\delta = 7.26$  ppm;  $^{13}\text{C}$ ,  $\delta = 77.16$  ppm), and the coupling constants ( $J$ ) are reported in hertz (Hz). Optical rotations were measured on a Perkin-Elmer Polarimeter 343 at 589 nm (Na D-line), and specific rotations are reported in  $10^{-1}$  deg  $\text{cm}^2 \text{g}^{-1}$ . Microwave reactions were performed using a Biotage Initiator system under reaction conditions as indicated for each individual reaction.

Reactions were monitored by TLC and LCMS to determine consumption of starting materials.

Flash column chromatography was performed using an Isolera Spektra One/Four purification

1  
2 system and the appropriately sized Biotage SNAP column containing KP-silica gel (50  $\mu\text{m}$ ).  
3  
4 Solvents are reported as volume/volume eluent mixture where applicable.  
5

6 High resolution mass spectra (HRMS) were recorded using a Waters LCT Premier Time of  
7 Flight (TOF) mass spectrometer or a Micromass Quadrupole-Time of Flight (Q-TOF)  
8 spectrometer.  
9  
10

11 Liquid chromatography mass spectrometry (LCMS) was carried out using an Ultra Performance  
12 Liquid Chromatographic system (UPLC) Waters Acquity H-class coupled to a Waters SQ Mass  
13 Spectrometer detector. Samples were detected using a Waters Acquity TUV detector at 2  
14 wavelengths (254 and 280 nm). Samples were run using an Acquity UPLC HSS column and a  
15 flow rate of 0.8 mL/min. The eluent consisted of 0.1% formic acid in water (A) and acetonitrile  
16 (B); gradient, from 95% A to 5% A over a period of 4 or 7 min.  
17  
18  
19  
20  
21  
22  
23

24 All final compounds had a purity greater than 95% by LCMS analysis.  
25  
26  
27

#### 28 **General Method A: Synthesis of thioacetamides 20–25, 29, and 32.**

29  
30 To a solution of the 2-chloroacetamide derivative (0.17 mmol) in MeOH (8 mL), 4-(4-  
31 bromophenyl)-1*H*-imidazole-2-thiol or 4-phenyl-1*H*-imidazole-2-thiol (0.17 mmol) was added,  
32 followed by a solution of NaOH (0.67 mmol) in H<sub>2</sub>O (2.5 mL). The reaction mixture was stirred  
33 at 70 °C for 3h. After cooling to rt, the solvents were removed *in vacuo* and the resulting residue  
34 was taken up in 30 mL of EtOAc and washed with H<sub>2</sub>O (15 mL). The aqueous layer was  
35 extracted with EtOAc (3  $\times$  30 mL) and the combined organic layers were washed with brine and  
36 dried over MgSO<sub>4</sub>. Filtration and evaporation afforded crude products, which were purified as  
37 indicated below.  
38  
39  
40  
41  
42  
43  
44  
45  
46  
47

#### 48 **General Method B: Synthesis of thioacetic derivatives 27 and 28.**

49  
50 A solution of 4-phenyl-1*H*-imidazole-2-thiol or 4-(4-bromophenyl)-1*H*-imidazole-2-thiol (2.80  
51 mmol) and NaOH (5.0 mmol) in EtOH (5 mL) was reflux for 1 h. After cooling to rt, a solution  
52 of 2-chloroacetic acid (2.80 mmol) in EtOH (2 mL) was added. The reaction was stirred at  
53 reflux for an additional 3 h, and then cooled to 0 °C. The reaction mixture was diluted with cold  
54  
55  
56  
57  
58  
59  
60

1  
2  
3 water (5 mL) and acidified with 1M HCl. The precipitated product was collected by filtration  
4  
5 and washed with DCM (2 x 2 mL).  
6  
7

8  
9 **General Method C: Synthesis of compounds 31, 33, and 36–39.**

10 A mixture of acid **59** (0.20 mmol) and SOCl<sub>2</sub> (2 ml) were heated at 80 °C for 2 h. The solvent  
11  
12 was removed under reduced pressure to give the acid chloride **60** as a white solid, which was  
13  
14 immediately dissolved in anhydrous DCM and it was added slowly dropwise at 0 °C to a  
15  
16 solution of the corresponding substituted 2-Aminoimidazoles (0.20 mmol) and TEA (0.80  
17  
18 mmol) in anhydrous DCM (5 mL). The reaction mixture was stirred at 40 °C for 36 h, and then  
19  
20 diluted with DCM (20 mL) and washed with saturated aqueous NaHCO<sub>3</sub>. The aqueous phase  
21  
22 layer was then extracted with DCM (2 x 20 mL), and the combined organic layers were dried  
23  
24 over MgSO<sub>4</sub>, filtered and the solvent was removed under reduced pressure to afford a yellow  
25  
26 oil, which was purified by flash chromatography eluting with the solvent system specified.  
27  
28  
29

30  
31 **General Method D: Synthesis of amides 34–35.**

32 A mixture of acid **59** (0.20 mmol) and SOCl<sub>2</sub> (2 mL) were heated at 80 °C for 2 h. The solvent  
33  
34 was removed under reduced pressure to give **60** as a white solid, which was immediately  
35  
36 dissolved in anhydrous DCM and it was added slowly dropwise at 0 °C to a solution of the  
37  
38 corresponding aniline (0.20 mmol) and triethylamine (0.80 mmol) in anhydrous DCM (5 mL).  
39  
40 The reaction mixture was stirred at rt for 4 h, and then diluted with DCM (20 mL) and washed  
41  
42 with saturated aqueous NaHCO<sub>3</sub>. The aqueous phase layer was then extracted with DCM (2 x  
43  
44 20 mL), and the combined organic layers were dried over MgSO<sub>4</sub>, filtered ant the solvent was  
45  
46 removed under reduced pressure to afford a yellow oil, which was purified by flash  
47  
48 chromatography eluting with the solvent system specified.  
49  
50  
51

52  
53 **General Method E: Synthesis of  $\alpha$ -chloroacetamides 40–43.**

54 Et<sub>3</sub>N (4.77 mmol) followed by a solution of chloroacetyl chloride (4.77 mmol) in DCM (3 mL)  
55  
56 were added to a stirred solution of the corresponding aniline (4.38 mmol) in DCM (5 mL) at rt.  
57  
58  
59  
60

1  
2  
3 The reaction mixture was stirred at rt for 2 – 4 h. The reaction was then diluted with DCM (20  
4 mL) and washed with saturated aqueous NaHCO<sub>3</sub>, 1M HCl and brine, dried over anhydrous  
5 MgSO<sub>4</sub>, and the solvent was removed under reduced pressure. Compound **43** was purified by  
6 flash chromatography eluting with the solvent system specified, although other analogues were  
7 used in subsequent reactions without further purification.  
8  
9  
10  
11  
12  
13

#### 14 **General Method F: Synthesis of Substituted *N*-(1*H*-imidazol-2-yl)acetamides 45–49.**

15  
16 A mixture of the corresponding 2-bromoacetophenone derivative (0.38 mmol) and  
17 acetylguanidine (1.13 mmol) in anhydrous acetonitrile (3 mL) was heated at 100 °C using  
18 microwave irradiation for 15 min. The solvent was removed, and the residue was taken in H<sub>2</sub>O  
19 (3 mL), filtered and the solid was washed with H<sub>2</sub>O (2 mL x 2) and DCM (2 mL). The solid  
20 obtained was used in the next step without further purification.  
21  
22  
23  
24  
25  
26  
27

#### 28 **General Method G: Synthesis of Substituted 2-Aminoimidazoles 50–54.**

29  
30 To a solution of the corresponding substituted *N*-(1*H*-imidazol-2-yl)acetamides (0.31 mmol) in  
31 a 1:1 v/v mixture of MeOH and H<sub>2</sub>O (2.4 mL) was added concentrated H<sub>2</sub>SO<sub>4</sub> (0.6 mL) and the  
32 reaction mixture was heated at 100 °C under microwave irradiation for 15–30 min. The reaction  
33 mixture was concentrated, and the resulting residue was resuspended in H<sub>2</sub>O (5 mL) and a  
34 saturated aqueous Na<sub>2</sub>CO<sub>3</sub> was added until pH 8. The product was extracted into EtOAc (3 x 40  
35 mL). The combined organic fractions were dried over MgSO<sub>4</sub>, and the solvent was removed  
36 under reduced pressure. The resulting solid was used in the next reaction without further  
37 purification.  
38  
39  
40  
41  
42  
43  
44  
45  
46  
47

48 **2-((4-(4-bromophenyl)-1*H*-imidazol-2-yl)thio)-*N*-phenylacetamide (20).** Compound **40** (29  
49 mg, 0.17 mmol) was reacted with 4-(4-bromophenyl)-1*H*-imidazole-2-thiol (43 mg, 0.17 mmol)  
50 according to the general method A. Purification by flash chromatography (1–20% v/v MeOH in  
51 DCM) afforded **20** (59 mg, 0.15 mmol, 89% yield) as a white solid. <sup>1</sup>H NMR (400 MHz,  
52 MeOD) δ 7.62 (br s, 2H), 7.56 – 7.39 (m, 5H), 7.36 – 7.17 (m, 2H), 7.13 – 7.00 (m, 1H), 3.82  
53  
54  
55  
56  
57  
58  
59  
60

(s, 2H) ppm.  $^{13}\text{C}$  NMR (100 MHz, MeOD)  $\delta$  169.6, 141.3, 139.6, 132.8, 129.8, 129.8, 127.5, 125.5, 121.4, 121.2, 121.2, 116.7, 39.6 ppm. LCMS (ESI $^-$ )  $m/z$  388.0 [ $\text{M} - \text{H}$ ] $^-$ , retention time 2.20 min (100%). HRMS (ESI $^+$ ):  $m/z$  calculated for  $\text{C}_{17}\text{H}_{15}\text{BrN}_3\text{OS}$  [ $\text{M} + \text{H}$ ] $^+$ : 388.0119. Found: 388.0121.

***N*-(benzofuran-5-yl)-2-((4-(4-bromophenyl)-1*H*-imidazol-2-yl)thio)acetamide (21).**

Compound **41** (36 mg, 0.17 mmol) was reacted with 4-(4-bromophenyl)-1*H*-imidazole-2-thiol (43 mg, 0.17 mmol) according to the general method A. Purification by flash chromatography (1–20% v/v MeOH in DCM) afforded **21** (70 mg, 0.16 mmol, 96% yield) as a white solid.  $^1\text{H}$  NMR (400 MHz, DMSO- $d_6$ )  $\delta$  12.50 (br s, 1H), 10.35 (br s, 1H), 7.94 (dd,  $J = 10.6, 2.0$  Hz, 2H), 7.73 – 7.64 (m, 2H), 7.52 – 7.44 (m, 4H), 7.34 (dd,  $J = 8.8, 2.2$  Hz, 1H), 6.91 (dd,  $J = 2.2, 1.0$  Hz, 1H), 3.99 (s, 2H) ppm.  $^{13}\text{C}$  NMR (100 MHz, DMSO- $d_6$ )  $\delta$  166.5, 150.8, 146.7, 140.2, 139.9, 134.3, 133.6, 131.4, 127.4, 126.2, 119.0, 116.9, 115.7, 111.6, 111.3, 107.0, 37.9. LCMS (ESI $^-$ )  $m/z$  428.0 [ $\text{M} - \text{H}$ ] $^-$ , retention time 2.22 min (100%). HRMS (ESI $^+$ ):  $m/z$  calculated for  $\text{C}_{19}\text{H}_{15}\text{BrN}_3\text{O}_2\text{S}$  [ $\text{M} + \text{H}$ ] $^+$ : 428.0068. Found: 428.0065.

**2-((4-(4-bromophenyl)-1*H*-imidazol-2-yl)thio)-*N*-(4-iodophenyl)acetamide (22).** Compound **42** (50 mg, 0.17 mmol) was reacted with 4-(4-bromophenyl)-1*H*-imidazole-2-thiol (43 mg, 0.17 mmol) according to the general method A. Purification by flash chromatography (1–20% v/v MeOH in DCM) afforded **22** (60 mg, 0.11 mmol, 69% yield) as a white solid.  $^1\text{H}$  NMR (500 MHz, MeOD)  $\delta$  7.63 – 7.58 (m, 4H), 7.56 – 7.45 (m, 3H), 7.38 – 7.31 (m, 2H), 3.81 (s, 2H) ppm.  $^{13}\text{C}$  NMR (125 MHz, MeOD)  $\delta$  169.6, 139.6, 138.9, 132.7, 127.5, 127.1, 123.0, 116.6, 111.4, 88.1, 39.7 ppm. LCMS (ESI $^-$ )  $m/z$  511.7 [ $\text{M} - \text{H}$ ] $^-$ , retention time 2.30 min (100%). HRMS (ESI $^+$ ):  $m/z$  calculated for  $\text{C}_{17}\text{H}_{14}\text{BrIN}_3\text{OS}$  [ $\text{M} + \text{H}$ ] $^+$ : 513.9086. Found: 513.9087.

***N*-phenyl-2-((4-phenyl-1*H*-imidazol-2-yl)thio)acetamide (23).** Compound **40** (42 mg, 0.25 mmol) was reacted with 4-phenyl-1*H*-imidazole-2-thiol (44 mg, 0.25 mmol) according to the general method A. Purification by flash chromatography (1–20% v/v MeOH in DCM) afforded

1  
2  
3 **23** (61 mg, 0.20 mmol, 82% yield) as a white solid.  $^1\text{H}$  NMR (500 MHz, MeOD)  $\delta$  7.71 (brs,  
4 2H), 7.54 – 7.49 (m, 2H), 7.47 (brs, 1H), 7.35 (t,  $J = 7.4$  Hz, 2H), 7.31 – 7.20 (m, 3H), 7.11 –  
5 7.03 (m, 1H), 3.83 (s, 2H) ppm.  $^{13}\text{C}$  NMR (125 MHz, MeOD)  $\delta$  168.3, 142.7, 139.5, 138.5,  
6 138.2, 128.4, 128.3, 126.7, 124.4, 124.1, 123.7, 119.8, 38.3 ppm. LCMS (ESI $^-$ )  $m/z$  308.0 [ $\text{M} -$   
7  $\text{H}]^-$ , retention time 1.82 min (95%). HRMS (ESI $^+$ ):  $m/z$  calculated for  $\text{C}_{17}\text{H}_{16}\text{N}_3\text{OS}$  [ $\text{M} + \text{H}]^+$ :  
8 310.1014. Found: 310.1004.  
9  
10  
11  
12  
13  
14  
15

16  
17 ***N*-(benzofuran-5-yl)-2-((4-phenyl-1*H*-imidazol-2-yl)thio)acetamide (24)**. Compound **41** (36  
18 mg, 0.17 mmol) was reacted with 4-phenyl-1*H*-imidazole-2-thiol (30 mg, 0.17 mmol) according  
19 to the general method A. Purification by flash chromatography (1–20% v/v MeOH in DCM)  
20 afforded **24** (42 mg, 0.12 mmol, 70% yield) as a white solid.  $^1\text{H}$  NMR (500 MHz, MeOD)  $\delta$   
21 7.87 (d,  $J = 2.1$  Hz, 1H), 7.72 (d,  $J = 2.2$  Hz, 1H), 7.68 (d,  $J = 7.7$  Hz, 2H), 7.46 (br s, 1H), 7.40  
22 (d,  $J = 8.8$  Hz, 1H), 7.37 – 7.29 (m, 3H), 7.23 (t,  $J = 7.4$  Hz, 1H), 6.76 (dd,  $J = 2.2, 0.9$  Hz, 1H),  
23 3.84 (s, 2H) ppm.  $^{13}\text{C}$  NMR (125 MHz, MeOD)  $\delta$  169.6, 153.5, 147.4, 140.9, 134.7, 129.8,  
24 129.1, 128.1, 125.8, 118.9, 114.2, 112.1, 107.7, 39.7 ppm. LCMS (ESI $^-$ )  $m/z$  348.0 [ $\text{M} - \text{H}]^-$ ,  
25 retention time 1.81 min (100 %). HRMS (ESI $^+$ ):  $m/z$  calculated for  $\text{C}_{19}\text{H}_{16}\text{N}_3\text{O}_2\text{S}$  [ $\text{M} + \text{H}]^+$ :  
26 350.0963. Found: 350.0971.  
27  
28  
29  
30  
31  
32  
33  
34  
35  
36  
37

38  
39 ***N*-(4-iodophenyl)-2-((4-phenyl-1*H*-imidazol-2-yl)thio)acetamide (25)**. Compound **42** (74 mg,  
40 0.25 mmol) was reacted with 4-phenyl-1*H*-imidazole-2-thiol (44 mg, 0.25 mmol) according to  
41 the general method A. Purification by flash chromatography (1–20% v/v MeOH in DCM)  
42 afforded **25** (70 mg, 0.16 mmol, 70% yield) as a white solid.  $^1\text{H}$  NMR (500 MHz, MeOD)  $\delta$   
43 7.66 (d,  $J = 7.7$  Hz, 2H), 7.61 – 7.54 (m, 2H), 7.44 (br s, 1H), 7.38 – 7.31 (m, 4H), 7.23 (t,  $J =$   
44 6.7 Hz, 1H), 3.80 (s, 2H) ppm.  $^{13}\text{C}$  NMR (125 MHz, MeOD)  $\delta$  169.7, 140.8, 139.6, 138.9,  
45 129.8, 128.2, 125.8, 123.0, 88.1, 39.8 ppm. LCMS (ESI $^-$ )  $m/z$  433.9 [ $\text{M} - \text{H}]^-$ , retention time  
46 2.13 min (98%). HRMS (ESI $^+$ ):  $m/z$  calculated for  $\text{C}_{17}\text{H}_{15}\text{IN}_3\text{OS}$  [ $\text{M} + \text{H}]^+$ : 435.9981. Found:  
47 435.9989.  
48  
49  
50  
51  
52  
53  
54  
55  
56  
57  
58  
59  
60

***N*-isopropyl-2-((4-phenyl-1*H*-imidazol-2-yl)thio)acetamide (26).** A solution of propan-2-amine (22  $\mu$ L, 0.25 mmol), 2-((4-phenyl-1*H*-imidazol-2-yl)thio)acetic acid (60 mg, 0.25 mmol), HATU (194 mg, 0.50 mmol), DIPEA (90  $\mu$ L, 0.50 mmol) in EtOAc (10 mL) was stirred for 5 h at rt. The reaction mixture was diluted with EtOAc (40 mL) and washed with saturated aqueous NaHCO<sub>3</sub> (20 mL), water (20 mL) and brine (20 mL). The organic layer was dried over MgSO<sub>4</sub> and filtered. The solvent was removed under reduced pressure to give an oil residue, which was purified by flash chromatography (5–100% v/v EtOAc in petroleum ether) to give the desired product as a white solid (50 mg, 0.18 mmol, 73% yield). <sup>1</sup>H NMR (500 MHz, MeOD)  $\delta$  7.37 (d,  $J$  = 7.8 Hz, 2H), 7.14 (s, 1H), 7.05 (t,  $J$  = 7.7 Hz, 2H), 6.93 (t,  $J$  = 7.4 Hz, 1H), 3.62 (dt,  $J$  = 13.1, 6.4 Hz, 1H), 3.00 (s, 2H), 0.78 (d,  $J$  = 6.6 Hz, 6H) ppm. <sup>13</sup>C NMR (125 MHz, MeOD)  $\delta$  170.3, 141.1, 140.8, 133.7, 129.7, 128.1, 125.7, 119.7, 43.0, 38.8, 22.4 ppm. LCMS (ESI<sup>-</sup>)  $m/z$  273.9 [M – H]<sup>-</sup>, retention time 1.52 min (100%). HRMS (ESI<sup>+</sup>):  $m/z$  calculated for C<sub>14</sub>H<sub>18</sub>N<sub>3</sub>OS [M + H]<sup>+</sup>: 276.1171. Found: 276.1172.

**2-((4-(4-bromophenyl)-1*H*-imidazol-2-yl)thio)acetic acid (27).** Following the general procedure B, from 4-(4-bromophenyl)-1*H*-imidazole-2-thiol (250 mg, 0.98 mmol) was obtained **27** (220 mg, 0.70 mmol, 72% yield) as a white solid. <sup>1</sup>H NMR (400 MHz, MeOD)  $\delta$  7.65 – 7.56 (m, 2H), 7.57 – 7.39 (m, 3H), 3.80 (s, 2H) ppm. <sup>13</sup>C NMR (100 MHz, MeOD)  $\delta$  172.9, 141.9, 140.2, 132.9, 132.6, 127.5, 121.8, 118.9, 37.4 ppm. LCMS (ESI<sup>-</sup>)  $m/z$  311.0 [M – H]<sup>-</sup>, retention time 1.59 min (98%). HRMS (ESI<sup>+</sup>):  $m/z$  calculated for C<sub>11</sub>H<sub>10</sub>BrN<sub>2</sub>O<sub>2</sub>S [M + H]<sup>+</sup>: 312.9646. Found: 312.9654.

**2-((4-phenyl-1*H*-imidazol-2-yl)thio)acetic acid (28).** Following the general procedure B, from 4-phenyl-1*H*-imidazole-2-thiol (500 mg, 2.80 mmol) was obtained **28** (450 mg, 1.92 mmol, 69% yield) as a white solid. <sup>1</sup>H NMR (500 MHz, MeOD)  $\delta$  7.68 (d,  $J$  = 7.2 Hz, 2H), 7.59 (s, 1H), 7.41 (t,  $J$  = 7.7 Hz, 2H), 7.32 (t,  $J$  = 7.4 Hz, 1H), 3.86 (s, 2H) ppm. <sup>13</sup>C NMR (125 MHz, MeOD)  $\delta$  172.7, 141.7, 139.6, 131.6, 130.0, 129.1, 126.0, 118.9, 37.5 ppm. LCMS (ESI<sup>+</sup>)  $m/z$

235.1 [M + H]<sup>+</sup>, retention time 1.22 min (100%). HRMS (ESI<sup>+</sup>): m/z calculated for C<sub>11</sub>H<sub>11</sub>N<sub>2</sub>O<sub>2</sub>S [M + H]<sup>+</sup>: 235.0541. Found: 235.0536.

***N*-(4-(1*H*-imidazol-4-yl)phenyl)-2-((4-(4-bromophenyl)-1*H*-imidazol-2-yl)thio)acetamide**

**(29)**. Compound **43** (40 mg, 0.17 mmol) was reacted with 4-(4-bromophenyl)-1*H*-imidazole-2-thiol (43 mg, 0.17 mmol) according to the general method A. Purification by flash chromatography (1–20% v/v MeOH in DCM) afforded **29** (51 mg, 0.12 mmol, 69% yield) as a white solid. <sup>1</sup>H NMR (400 MHz, MeOD) δ 7.72 (d, *J* = 1.1 Hz, 1H), 7.66 (d, *J* = 8.5 Hz, 4H), 7.59 – 7.47 (m, 5H), 7.40 (br s, 1H), 3.86 (s, 2H) ppm. <sup>13</sup>C NMR (125 MHz, MeOD) δ 169.4, 141.2, 138.4, 137.0, 132.8, 127.5, 126.2, 121.4, 116.7, 111.4, 39.7 ppm. LCMS (ESI<sup>–</sup>) m/z 451.9 [M – H]<sup>–</sup>, retention time 1.65 min (100%). HRMS (ESI<sup>+</sup>): m/z calculated for C<sub>20</sub>H<sub>17</sub>BrN<sub>5</sub>OS [M + H]<sup>+</sup>: 454.0337. Found: 454.0334.

**1-(4-(1*H*-imidazol-4-yl)phenyl)-3-((5-(4-bromophenyl)-1*H*-imidazol-2-yl)methyl)urea (30)**

To a solution of 4-(1*H*-imidazol-4-yl)aniline (50 mg, 0.31 mmol) in THF (5 mL) was added 1,1-carbonyldiimidazole (76 mg, 0.47 mmol). The mixture was stirred at rt overnight, and then it was filtered. The filter was washed with THF (2 x 3 mL) and the resulting solid (30 mg, 0.12 mmol) was dissolved in DMF (3 mL), **44** (42 mg, 0.12 mmol) and *N,N*-diisopropylethylamine (74 μL, 0.48 mmol) were added. The reaction mixture was stirred at rt for 14 h, and then it was poured into water, extracted with EtOAc, dried over Na<sub>2</sub>SO<sub>4</sub>, and concentrated. After cooling to 0°C, a 1:5 v/v mixture of MeOH and DCM (12 mL) was added and the suspended solid was collected by filtration and dried at vacuum to yield **30** (35 mg, 0.08 mmol, 26% yield) as a white solid. <sup>1</sup>H NMR (500 MHz, DMSO-*d*<sub>6</sub>) δ 12.03 (br s, 2H), 8.64 (br s, 1H), 7.73 – 7.68 (m, 2H), 7.64 – 7.59 (m, 2H), 7.57 (d, *J* = 1.9 Hz, 1H), 7.52 – 7.47 (m, 2H), 7.47 – 7.39 (m, 2H), 7.39 – 7.32 (m, 2H), 6.58 (br s, 1H), 4.33 (d, *J* = 5.5 Hz, 2H) ppm. <sup>13</sup>C NMR (125 MHz, DMSO-*d*<sub>6</sub>) δ 155.5, 146.9, 140.6, 138.9, 138.9, 135.9, 134.6, 131.7, 128.8, 126.6, 125.1, 125.0, 119.0, 118.4, 118.2, 113.7, 111.7, 37.6 ppm. LCMS (ESI<sup>–</sup>) m/z 437.0 [M – H]<sup>–</sup>, retention time 5.07 min (97%). HRMS (ESI<sup>+</sup>): m/z calculated for C<sub>20</sub>H<sub>18</sub>BrN<sub>6</sub>O [M + H]<sup>+</sup>: 437.0725. Found: 437.0725.

1  
2  
3 ***N*-(4-(4-bromophenyl)-1*H*-imidazol-2-yl)-2-(4-(1-methyl-1*H*-imidazol-4-**  
4 **yl)phenoxy)propanamide (31).** 4-(4-bromophenyl)-1*H*-imidazol-2-amine **50** (48 mg, 0.20  
5 mmol) was reacted with the acid chloride **60** (53 mg, 0.20 mmol) and Et<sub>3</sub>N (112 μL, 0.80 mmol)  
6 according to the general method C. The crude product was purified by flash chromatography  
7 (0–20% v/v MeOH in DCM) to give compound **31** as a white solid (64 mg, 0.14 mmol, 67%  
8 yield). <sup>1</sup>H NMR (500 MHz, CDCl<sub>3</sub>) δ 10.79 (br s, 1H), 9.49 (br s, 1H), 7.69 (d, *J* = 8.7 Hz, 2H),  
9 7.58 – 7.41 (m, 5H), 7.18 – 6.97 (m, 2H), 6.93 (d, *J* = 8.8 Hz, 2H), 4.86 (d, *J* = 6.8 Hz, 1H),  
10 3.71 (s, 3H), 1.65 (d, *J* = 6.7 Hz, 3H) ppm. <sup>13</sup>C NMR (125 MHz, CDCl<sub>3</sub>) δ 171.5, 155.2, 141.8,  
11 141.2, 138.0, 137.2, 131.7, 129.1, 127.6, 126.3, 120.5, 115.8, 115.6, 115.3, 108.1, 74.6, 33.5,  
12 18.5 ppm. LCMS (ESI+) *m/z* 465.9 [M + H]<sup>+</sup>, retention time 2.73 min (95%). HRMS (ESI+):  
13 *m/z* calculated for C<sub>22</sub>H<sub>21</sub>BrN<sub>5</sub>O<sub>2</sub> [M + H]<sup>+</sup>: 466.0879. Found: 466.0874. ((**S**)-**31**): 69% yield.  
14 [α]<sub>D</sub><sup>25</sup> –40.2 (*c* 1.0, CHCl<sub>3</sub>). LCMS (ESI+) *m/z* 466.0 [M + H]<sup>+</sup>, retention time 2.70 min (95%).  
15 HRMS (ESI+): *m/z* calculated for C<sub>22</sub>H<sub>21</sub>BrN<sub>5</sub>O<sub>2</sub> [M + H]<sup>+</sup>: 466.0879. Found: 466.0879.  
16  
17  
18  
19  
20  
21  
22  
23  
24  
25  
26  
27  
28  
29

30  
31 ***N*-(4-(1*H*-imidazol-4-yl)phenyl)-2-((4-phenyl-1*H*-imidazol-2-yl)thio)acetamide (32).**  
32 Compound **43** (40 mg, 0.17 mmol) was reacted with 4-(4-bromophenyl)-1*H*-imidazole-2-thiol  
33 (30 mg, 0.17 mmol) according to the general method A. Purification by flash chromatography  
34 (1–20% v/v MeOH in DCM) afforded **32** (41 mg, 0.11 mmol, 65% yield) as a white solid. <sup>1</sup>H  
35 NMR (400 MHz, DMSO-*d*<sub>6</sub>) δ 12.46 (br s, 2H), 10.42 (br s, 1H), 7.76 (br s, 2H), 7.68 (d, *J* =  
36 8.2 Hz, 4H), 7.56 (d, *J* = 8.5 Hz, 2H), 7.52 (s, 1H), 7.34 (br s, 2H), 7.19 (br s, 1H), 3.99 (s, 2H)  
37 ppm. <sup>13</sup>C NMR (125 MHz, DMSO-*d*<sub>6</sub>) δ 167.0, 141.7, 139.9, 137.7, 136.2, 134.6, 128.9, 126.7,  
38 125.2, 124.6, 119.7, 115.4, 39.5 ppm. LCMS (ESI+) *m/z* 376.1 [M + H]<sup>+</sup>, retention time 0.88  
39 min (100%). HRMS (ESI+): *m/z* calculated for C<sub>20</sub>H<sub>18</sub>N<sub>5</sub>OS [M + H]<sup>+</sup>: 376.1232. Found:  
40 376.1241.  
41  
42  
43  
44  
45  
46  
47  
48  
49  
50  
51

52  
53 ***N*-(4-(4-bromophenyl)oxazol-2-yl)-2-(4-(1-methyl-1*H*-imidazol-4-yl)phenoxy)propanamide**  
54 **(33).** 4-(4-bromophenyl)oxazol-2-amine **61** (39 mg, 0.16 mmol) was reacted with the acid  
55 chloride **60** (43 mg, 0.16 mmol) and Et<sub>3</sub>N (90 μL, 0.64 mmol) according to the general method  
56  
57  
58  
59  
60

C. The crude product was purified by flash chromatography (0–15% v/v MeOH in DCM) to give compound **33** as a white solid (49 mg, 0.10 mmol, 64% yield). <sup>1</sup>H NMR (400 MHz, CDCl<sub>3</sub>) δ 9.13 (br s, 1H), 7.81 – 7.66 (m, 3H), 7.63 – 7.50 (m, 4H), 7.47 (s, 1H), 7.13 (d, *J* = 1.3 Hz, 1H), 7.03 – 6.94 (m, 2H), 4.90 (q, *J* = 6.6 Hz, 1H), 3.74 (s, 3H), 1.70 (d, *J* = 6.8 Hz, 3H) ppm. <sup>13</sup>C NMR (101 MHz, CDCl<sub>3</sub>) δ 155.1, 141.7, 138.0, 131.9, 131.7, 130.3, 129.4, 129.3, 127.8, 127.0, 126.7, 126.4, 122.2, 116.0, 115.4, 75.1, 33.5, 18.4 ppm. LCMS (ESI+) *m/z* 468.9 [M + H]<sup>+</sup>, retention time 2.86 min (95%). HRMS (ESI+): *m/z* calculated for C<sub>22</sub>H<sub>20</sub>BrN<sub>4</sub>O<sub>3</sub> [M + H]<sup>+</sup>: 467.0719. Found: 467.0711.

**2-(4-(1-methyl-1*H*-imidazol-4-yl)phenoxy)-*N*-phenylpropanamide (34).** Aniline (28 μL, 0.30 mmol) was reacted with the acid chloride **60** (53 mg, 0.20 mmol) and Et<sub>3</sub>N (112 μL, 0.80 mmol) according to the general method D. The crude product was purified by flash chromatography (0–20% v/v MeOH in DCM) to give compound **34** as a white solid (48 mg, 0.14 mmol, 74% yield). <sup>1</sup>H NMR (400 MHz, CDCl<sub>3</sub>) δ 8.25 (br s, 1H), 7.79 – 7.69 (m, 2H), 7.60 – 7.52 (m, 2H), 7.47 (d, *J* = 1.3 Hz, 1H), 7.35 (dd, *J* = 8.5, 7.3 Hz, 2H), 7.19 – 7.06 (m, 2H), 7.05 – 6.97 (m, 2H), 4.82 (q, *J* = 6.7 Hz, 1H), 3.73 (s, 3H), 1.69 (d, *J* = 6.8 Hz, 3H) ppm. <sup>13</sup>C NMR (100 MHz, CDCl<sub>3</sub>) δ 170.3, 155.6, 141.8, 137.9, 137.0, 129.0, 129.0, 126.3, 124.7, 120.0, 116.0, 115.3, 75.6, 33.5, 18.7 ppm. LCMS (ESI+) *m/z* 322.2 [M + H]<sup>+</sup>, retention time 1.86 min (97%). HRMS (ESI+): *m/z* calculated for C<sub>19</sub>H<sub>20</sub>N<sub>3</sub>O<sub>2</sub> [M + H]<sup>+</sup>: 322.1556. Found: 322.1552.

***N*-(4-iodophenyl)-2-(4-(1-methyl-1*H*-imidazol-4-yl)phenoxy)propanamide (35).** 4-iodoaniline (65 mg, 0.30 mmol) was reacted with the acid chloride **60** (53 mg, 0.20 mmol) and Et<sub>3</sub>N (112 μL, 0.80 mmol) according to the general method D. The crude product was purified by flash chromatography (0–20% v/v MeOH in DCM) to give compound **35** as a pink solid (62 mg, 0.14 mmol, 68% yield). <sup>1</sup>H NMR (400 MHz, CDCl<sub>3</sub>) δ 8.28 (br s, 1H), 7.77 – 7.69 (m, 2H), 7.69 – 7.57 (m, 2H), 7.47 (d, *J* = 1.4 Hz, 1H), 7.41 – 7.31 (m, 2H), 7.11 (d, *J* = 1.3 Hz, 1H), 7.03 – 6.91 (m, 2H), 4.80 (q, *J* = 6.7 Hz, 1H), 3.73 (s, 3H), 1.67 (d, *J* = 6.8 Hz, 3H) ppm. <sup>13</sup>C NMR (100 MHz, CDCl<sub>3</sub>) δ 170.4, 155.5, 141.7, 137.9, 136.9, 129.0, 126.3, 126.0, 121.8, 116.0,

1  
2  
3 115.3, 87.9, 75.6, 33.5, 18.6 ppm. LCMS (ESI+)  $m/z$  448.2  $[M + H]^+$ , retention time 2.47 min  
4 (96%). HRMS (ESI+):  $m/z$  calculated for  $C_{19}H_{19}IN_3O_2$   $[M + H]^+$ : 448.0522. Found: 448.0517.  
5  
6  
7

8  
9 **2-(4-(1-methyl-1*H*-imidazol-4-yl)phenoxy)-*N*-(4-phenyl-1*H*-imidazol-2-yl)propanamide**

10  
11 **(36)**. 4-phenyl-1*H*-imidazol-2-amine **51** (33 mg, 0.20 mmol) was reacted with the acid chloride  
12 **60** (53 mg, 0.20 mmol) and  $Et_3N$  (112  $\mu$ L, 0.80 mmol) according to the general method C. The  
13 crude product was purified by flash chromatography (0–15% v/v MeOH in DCM) to give  
14 compound **36** as a brown solid (57 mg, 0.15 mmol, 72% yield).  $^1H$  NMR (400 MHz,  $CDCl_3$ )  $\delta$   
15 10.84 (br s, 1H), 9.51 (br s, 1H), 7.78 – 7.56 (m, 4H), 7.46 (d,  $J = 1.2$  Hz, 1H), 7.39 (t,  $J = 7.7$   
16 Hz, 2H), 7.22 – 7.26 (m, 1H), 7.14 (s, 1H), 7.11 (d,  $J = 1.4$  Hz, 1H), 7.02 – 6.89 (m, 2H), 4.89  
17 (q,  $J = 6.8$  Hz, 1H), 3.73 (s, 3H), 1.68 (d,  $J = 6.8$  Hz, 3H) ppm.  $^{13}C$  NMR (125 MHz,  $CDCl_3$ )  $\delta$   
18 171.3, 155.2, 141.8, 137.9, 129.1, 128.7, 126.9, 126.3, 124.6, 115.9, 115.3, 107.8, 74.5, 33.5,  
19 18.5 ppm. LCMS (ESI+)  $m/z$  388.1  $[M + H]^+$ , retention time 4.44 min (100%). HRMS (ESI+):  
20  $m/z$  calculated for  $C_{22}H_{22}N_5O_2$   $[M + H]^+$ : 388.1773. Found: 388.1767.  
21  
22  
23  
24  
25  
26  
27  
28  
29  
30  
31

32  
33 **2-(4-(1-methyl-1*H*-imidazol-4-yl)phenoxy)-*N*-(4-(4-morpholinophenyl)-1*H*-imidazol-2-**

34 **yl)propanamide (37)**. 4-(4-morpholinophenyl)-1*H*-imidazol-2-amine **52** (40 mg, 0.16 mmol)  
35 was reacted with the acid chloride **60** (43 mg, 0.16 mmol) and  $Et_3N$  (90  $\mu$ L, 0.65 mmol)  
36 according to the general method C. The crude product was purified by flash chromatography  
37 (3–15% v/v MeOH in DCM) to give compound **37** as a brown solid (51 mg, 0.11 mmol, 67%  
38 yield).  $^1H$  NMR (400 MHz,  $CDCl_3$ )  $\delta$  10.74 (br s, 1H), 7.71 (d,  $J = 8.8$  Hz, 2H), 7.54 (br s, 2H),  
39 7.47 (d,  $J = 1.4$  Hz, 1H), 7.11 (d,  $J = 1.4$  Hz, 1H), 7.03 – 6.88 (m, 5H), 4.90 (q,  $J = 6.7$  Hz, 1H),  
40 4.06 – 3.83 (m, 4H), 3.73 (s, 3H), 3.27 – 3.01 (m, 4H), 1.69 (d,  $J = 6.8$  Hz, 3H) ppm.  $^{13}C$  NMR  
41 (125 MHz,  $CDCl_3$ )  $\delta$  171.5, 155.3, 150.3, 141.8, 141.0, 137.9, 137.8, 128.9, 126.3, 125.5, 115.8,  
42 115.3, 74.4, 66.9, 49.3, 33.6, 18.7 ppm. LCMS (ESI+)  $m/z$  473.2  $[M + H]^+$ , retention time 2.22  
43 min (100%). HRMS (ESI+):  $m/z$  calculated for  $C_{26}H_{29}N_6O_3$   $[M + H]^+$ : 473.2301. Found:  
44 473.2297.  
45  
46  
47  
48  
49  
50  
51  
52  
53  
54  
55  
56  
57  
58  
59  
60

1  
2  
3 ***N*-(4-(4-methoxyphenyl)-1*H*-imidazol-2-yl)-2-(4-(1-methyl-1*H*-imidazol-4-**  
4 **yl)phenoxy)propanamide (38).** 4-(4-methoxyphenyl)-1*H*-imidazol-2-amine **53** (30 mg, 0.16  
5 mmol) was reacted with the acid chloride **60** (43 mg, 0.16 mmol) and Et<sub>3</sub>N (90 μL, 0.65 mmol)  
6 according to the general method C. The crude product was purified by flash chromatography  
7 (1–20% v/v MeOH in DCM) to give compound **38** as a yellow solid (45 mg, 0.11 mmol, 67%  
8 yield). <sup>1</sup>H NMR (400 MHz, CDCl<sub>3</sub>) δ 10.73 (br s, 1H), 9.62 (br s, 1H), 7.78 – 7.65 (m, 2H), 7.57  
9 (br s, 2H), 7.46 (d, *J* = 1.4 Hz, 1H), 7.10 (d, *J* = 1.3 Hz, 1H), 7.02 (s, 1H), 6.95 (dd, *J* = 10.5, 8.8  
10 Hz, 4H), 4.88 (q, *J* = 6.8 Hz, 1H), 3.84 (s, 3H), 3.73 (s, 3H), 1.68 (d, *J* = 6.8 Hz, 3H) ppm. <sup>13</sup>C  
11 NMR (125 MHz, CDCl<sub>3</sub>) δ 171.4, 158.7, 155.3, 141.8, 140.8, 137.9, 129.1, 126.3, 125.8, 115.8,  
12 115.3, 114.2, 74.7, 55.3, 33.4, 18.4 ppm. LCMS (ESI+) *m/z* 418.3 [M + H]<sup>+</sup>, retention time 4.69  
13 min (100%). HRMS (ESI+): *m/z* calculated for C<sub>23</sub>H<sub>24</sub>N<sub>5</sub>O<sub>3</sub> [M + H]<sup>+</sup>: 418.1879. Found:  
14 418.1875.  
15  
16  
17  
18  
19  
20  
21  
22  
23  
24  
25  
26  
27

28 ***N*-(4-(4-iodophenyl)-1*H*-imidazol-2-yl)-2-(4-(1-methyl-1*H*-imidazol-4-**  
29 **yl)phenoxy)propanamide (39).** 4-(4-iodophenyl)-1*H*-imidazol-2-amine **54** (46 mg, 0.16 mmol)  
30 was reacted with the acid chloride **60** (43 mg, 0.16 mmol) and Et<sub>3</sub>N (90 μL, 0.65 mmol)  
31 according to the general method C. The crude product was purified by flash chromatography  
32 (1–20% v/v MeOH in DCM) to give compound **39** as a yellow solid (50 mg, 0.10 mmol, 61%  
33 yield). <sup>1</sup>H NMR (500 MHz, CDCl<sub>3</sub>) δ 10.75 (br s, 1H), 9.42 (br s, 1H), 7.69 (t, *J* = 8.3 Hz, 4H),  
34 7.53 – 7.33 (m, 3H), 7.10 (d, *J* = 8.3 Hz, 2H), 6.95 (d, *J* = 8.9 Hz, 2H), 4.88 (q, *J* = 6.7 Hz, 1H),  
35 3.71 (s, 3H), 1.66 (d, *J* = 6.7 Hz, 3H) ppm. <sup>13</sup>C NMR (125 MHz, CDCl<sub>3</sub>) δ 171.5, 155.2, 141.7,  
36 138.0, 137.7, 129.1, 126.5, 126.3, 115.8, 115.3, 108.1, 91.8, 74.5, 33.5, 18.5 ppm. LCMS  
37 (ESI+) *m/z* 514.2 [M + H]<sup>+</sup>, retention time 4.61 min (95%). HRMS (ESI+): *m/z* calculated for  
38 C<sub>22</sub>H<sub>21</sub>I N<sub>5</sub>O<sub>2</sub> [M + H]<sup>+</sup>: 514.0740. Found: 514.0740.  
39  
40  
41  
42  
43  
44  
45  
46  
47  
48  
49  
50  
51

52 **2-chloro-*N*-phenylacetamide (40).** Aniline (400 μL, 4.38 mmol) was reacted with chloroacetyl  
53 chloride (380 μL, 4.77 mmol) and Et<sub>3</sub>N (670 μL, 4.77 mmol) according to the general method  
54 E, and used in subsequent reactions without further purification. Compound **40** was obtained  
55  
56  
57  
58  
59  
60

(720 mg, 4.24 mmol, 96% yield) as a green solid and was used without further purification.  $^1\text{H}$  NMR (400 MHz,  $\text{CDCl}_3$ )  $\delta$  8.27 (br s, 1H), 7.58 (d,  $J = 7.7$  Hz, 2H), 7.39 (t,  $J = 7.9$  Hz, 2H), 7.20 (t,  $J = 7.4$  Hz, 1H), 4.22 (s, 2H) ppm.  $^{13}\text{C}$  NMR (100 MHz,  $\text{CDCl}_3$ )  $\delta$  163.9, 136.8, 129.3, 125.4, 120.2, 43.0 ppm. LCMS (ESI+)  $m/z$  170.1  $[\text{M} + \text{H}]^+$ , retention time 1.58 min (100%). HRMS (ESI+):  $m/z$  calculated for  $\text{C}_8\text{H}_9\text{ClNO}$   $[\text{M} + \text{H}]^+$ : 170.0373. Found: 170.0366. NMR data is in accordance with literature values.<sup>39</sup>

***N*-(benzofuran-5-yl)-2-chloroacetamide (41)**. Benzofuran-5-amine (140 mg, 1.05 mmol) was reacted with chloroacetyl chloride (93  $\mu\text{L}$ , 1.16 mmol) and  $\text{Et}_3\text{N}$  (162  $\mu\text{L}$ , 1.16 mmol) according to the general method E, and used in subsequent reactions without further purification. Compound **41** was obtained (219 mg, 1.04 mmol, 99% yield) as a green solid and was used without further purification.  $^1\text{H}$  NMR (400 MHz,  $\text{CDCl}_3$ )  $\delta$  8.41 (br s, 1H), 7.94 (d,  $J = 2.2$  Hz, 1H), 7.64 (d,  $J = 2.2$  Hz, 1H), 7.47 (dd,  $J = 8.8, 0.8$  Hz, 1H), 7.32 (dd,  $J = 8.8, 2.2$  Hz, 1H), 6.76 (dd,  $J = 2.2, 0.9$  Hz, 1H), 4.23 (s, 2H) ppm.  $^{13}\text{C}$  NMR (100 MHz,  $\text{CDCl}_3$ )  $\delta$  163.9, 152.4, 146.1, 131.9, 127.9, 117.7, 113.3, 111.6, 106.8, 43.0 ppm. LCMS (ESI+)  $m/z$  210.1  $[\text{M} + \text{H}]^+$ , retention time 1.71 min (100%). HRMS (ESI+):  $m/z$  calculated for  $\text{C}_{11}\text{H}_9\text{ClNO}_2$   $[\text{M} + \text{H}]^+$ : 210.0322. Found: 210.0319.

**2-chloro-*N*-(4-iodophenyl)acetamide (42)**. 4-iodoaniline (500 mg, 2.28 mmol) was reacted with chloroacetyl chloride (200  $\mu\text{L}$ , 2.51 mmol) and  $\text{Et}_3\text{N}$  (350  $\mu\text{L}$ , 2.51 mmol) according to the general method E. The crude product was purified by flash chromatography (10–100% v/v EtOAc in petroleum ether) to give compound **42** as a brown solid (600 mg, 2.03 mmol, 89% yield).  $^1\text{H}$  NMR (400 MHz,  $\text{CDCl}_3$ )  $\delta$  8.32 – 8.11 (br s, 1H), 7.69 (d,  $J = 8.8$  Hz, 2H), 7.36 (d,  $J = 8.7$  Hz, 2H), 4.20 (s, 2H) ppm.  $^{13}\text{C}$  NMR (100 MHz,  $\text{CDCl}_3$ )  $\delta$  163.8, 138.1, 136.4, 121.8, 88.7, 42.9 ppm. LCMS (ESI-)  $m/z$  293.7  $[\text{M} - \text{H}]^-$ , retention time 2.38 min (100%). HRMS (ESI-):  $m/z$  calculated for  $\text{C}_8\text{H}_6\text{ClINO}$   $[\text{M} - \text{H}]^-$ : 293.9183. Found: 293.9187. NMR data is in accordance with literature values.<sup>40</sup>

1  
2  
3 ***N*-(4-(1*H*-imidazol-4-yl)phenyl)-2-chloroacetamide (43)**. 4-(1*H*-imidazol-4-yl)aniline (200  
4 mg, 1.25 mmol) was reacted with chloroacetyl chloride (109  $\mu$ L, 1.38 mmol) and Et<sub>3</sub>N (192  $\mu$ L,  
5 1.38 mmol) according to the general method E. The crude product was purified by flash  
6 chromatography (3–20% v/v MeOH in DCM) to give compound **43** as a yellow solid (264 mg,  
7 1.12 mmol, 89% yield). <sup>1</sup>H NMR (400 MHz, DMSO-*d*<sub>6</sub>)  $\delta$  10.43 (br s, 1H), 9.83 (br s, 1H), 7.98  
8 (br s, 1H), 7.77 – 7.65 (m, 2H), 7.70 – 7.47 (m, 3H), 4.27 (s, 2H) ppm. LCMS (ESI+) *m/z* 236.2  
9 [M + H]<sup>+</sup>, retention time 1.15 min (100%). HRMS (ESI+): *m/z* calculated for C<sub>11</sub>H<sub>10</sub>ClN<sub>3</sub>O [M  
10 + H]<sup>+</sup>: 236.0591. Found: 236.0590.  
11  
12  
13  
14  
15  
16  
17  
18  
19

20 **(5-(4-bromophenyl)-1*H*-imidazol-2-yl)methanamine hydrochloride (44)**. 4M HCl (2 mL)  
21 was added slowly to a stirred solution of benzyl ((5-(4-bromophenyl)-1*H*-imidazol-2-  
22 yl)methyl)carbamate<sup>36</sup> (105 mg, 0.26 mmol) in dioxane (1 mL). The mixture was stirred at 100  
23 °C for 4h, and then the solvents were removed under reduced pressure to give the desired  
24 product as a white solid (86 mg, 0.26 mmol, 100% yield). <sup>1</sup>H NMR (500 MHz, MeOD)  $\delta$  8.00  
25 (s, 1H), 7.75 – 7.67 (m, 4H), 4.55 (s, 2H) ppm. <sup>13</sup>C NMR (125 MHz, MeOD)  $\delta$  140.8, 136.0,  
26 133.7, 128.4, 127.6, 124.7, 117.8, 111.4, 34.8 ppm. LCMS (ESI-) *m/z* 250.1 [M – H]<sup>-</sup>, retention  
27 time 2.13 min (100%). HRMS (ESI-): *m/z* calculated for C<sub>10</sub>H<sub>9</sub>BrN<sub>3</sub> [M + H]<sup>+</sup>: 249.9980.  
28 Found: 249.9987.  
29  
30  
31  
32  
33  
34  
35  
36  
37  
38  
39

40 ***N*-(4-(4-bromophenyl)-1*H*-imidazol-2-yl)acetamide (45)**. Following the general method F,  
41 from 2-bromo-1-(4-bromophenyl)ethanone (104 mg, 0.38 mmol) was obtained **45** (88 mg, 0.31  
42 mmol, 84% yield) as a green solid. <sup>1</sup>H NMR (500 MHz, DMSO-*d*<sub>6</sub>)  $\delta$  11.66 (br s, 1H), 11.20  
43 (br s, 1H), 7.72 – 7.57 (m, 2H), 7.54 – 7.42 (m, 2H), 7.30 (d, *J* = 1.6 Hz, 1H), 2.05 (s, 3H) ppm.  
44 <sup>13</sup>C NMR (125 MHz, DMSO-*d*<sub>6</sub>)  $\delta$  169.0, 141.9, 135.5, 134.4, 131.7, 126.4, 119.0, 110.4, 23.3  
45 ppm. LCMS (ESI+) *m/z* 282.1 [M + H]<sup>+</sup>, retention time 2.13 min (100%). HRMS (ESI+): *m/z*  
46 calculated for C<sub>11</sub>H<sub>11</sub>BrN<sub>3</sub>O [M + H]<sup>+</sup>: 280.0085. Found: 280.0080. NMR data is in accordance  
47 with literature values.<sup>37</sup>  
48  
49  
50  
51  
52  
53  
54  
55  
56  
57  
58  
59  
60

1  
2  
3 ***N*-(4-phenyl-1*H*-imidazol-2-yl)acetamide (46)**. Following the general method F, from 2-  
4 bromo-1-phenylethan-1-one (100 mg, 0.50 mmol) was obtained **46** (79 mg, 0.39 mmol, 78%  
5 yield) as a green solid. <sup>1</sup>H NMR (400 MHz, DMSO-*d*<sub>6</sub>) δ 11.59 (br s, 1H), 11.24 (br s, 1H), 7.71  
6 (d, *J* = 7.6 Hz, 2H), 7.32 (t, *J* = 7.6 Hz, 2H), 7.25 (br s, 1H), 7.16 (t, *J* = 7.4 Hz, 1H), 2.07 (s,  
7 3H) ppm. <sup>13</sup>C NMR (100 MHz, DMSO-*d*<sub>6</sub>) δ 169.0, 141.7, 136.6, 128.9, 126.3, 124.4, 109.6,  
8 23.3 ppm. LCMS (ESI<sup>-</sup>) *m/z* 200.0 [M - H]<sup>-</sup>, retention time 1.44 min (100%). HRMS (ESI<sup>+</sup>):  
9 *m/z* calculated for C<sub>11</sub>H<sub>12</sub>N<sub>3</sub>O [M + H]<sup>+</sup>: 202.0980. Found: 202.0977. NMR data is in  
10 accordance with literature values.<sup>37</sup>  
11  
12  
13  
14  
15  
16  
17  
18  
19

20 ***N*-(4-(4-morpholinophenyl)-1*H*-imidazol-2-yl)acetamide (47)**. Following the general method  
21 F, from 2-bromo-1-(4-(piperidin-1-yl)phenyl)ethan-1-one (106 mg, 0.38 mmol) was obtained **47**  
22 (90 mg, 0.31 mmol, 83% yield) as a brown solid. <sup>1</sup>H NMR (500 MHz, DMSO-*d*<sub>6</sub>) δ 11.46 (br s,  
23 1H), 11.17 (br s, 1H), 7.55 (d, *J* = 8.2 Hz, 2H), 7.06 (br s, 1H), 6.89 (d, *J* = 8.5 Hz, 2H), 3.93 –  
24 3.53 (m, 4H), 3.07 (t, *J* = 4.8 Hz, 4H), 2.04 (s, 3H) ppm. <sup>13</sup>C NMR (126 MHz, DMSO-*d*<sub>6</sub>) δ  
25 168.8, 149.8, 141.4, 136.8, 125.2, 115.6, 113.5, 107.9, 66.6, 49.0, 23.2 ppm. LCMS (ESI<sup>-</sup>) *m/z*  
26 285.1 [M - H]<sup>-</sup>, retention time 1.60 min (95%). HRMS (ESI<sup>+</sup>): *m/z* calculated for C<sub>15</sub>H<sub>19</sub>N<sub>4</sub>O<sub>2</sub>  
27 [M + H]<sup>+</sup>: 287.1508. Found: 287.1505.  
28  
29  
30  
31  
32  
33  
34  
35  
36  
37

38 ***N*-(4-(4-methoxyphenyl)-1*H*-imidazol-2-yl)acetamide (48)**. Following the general method F,  
39 from 2-bromo-1-(4-methoxyphenyl)ethan-1-one (150 mg, 0.66 mmol) was obtained **48** (110  
40 mg, 0.47 mmol, 71% yield) as a white solid. <sup>1</sup>H NMR (400 MHz, DMSO-*d*<sub>6</sub>) δ 11.52 (br s, 1H),  
41 11.20 (br s, 1H), 7.62 (d, *J* = 8.1 Hz, 2H), 7.11 (s, 1H), 6.89 (d, *J* = 8.4 Hz, 2H), 3.75 (s, 3H),  
42 2.06 (s, 3H) ppm. <sup>13</sup>C NMR (100 MHz, DMSO-*d*<sub>6</sub>) δ 168.5, 157.8, 141.2, 136.1, 127.6, 125.3,  
43 113.9, 107.9, 55.1, 22.9 ppm. LCMS (ESI<sup>-</sup>) *m/z* 230.1 [M - H]<sup>-</sup>, retention time 1.52 min (96%).  
44 HRMS (ESI<sup>+</sup>): *m/z* calculated for C<sub>12</sub>H<sub>14</sub>N<sub>3</sub>O<sub>2</sub> [M + H]<sup>+</sup>: 232.1086. Found: 232.1082. NMR  
45 data is in accordance with literature values.<sup>37</sup>  
46  
47  
48  
49  
50  
51  
52  
53  
54  
55  
56  
57  
58  
59  
60

1  
2  
3 ***N*-(4-(4-iodophenyl)-1*H*-imidazol-2-yl)acetamide (49)**. Following the general method F, from  
4 2-bromo-1-(4-iodophenyl)ethan-1-one (214 mg, 0.66 mmol) was obtained **49** (190 mg, 0.58  
5 mmol, 88% yield) as a green solid. <sup>1</sup>H NMR (500 MHz, DMSO-*d*<sub>6</sub>) δ 11.66 (br s, 1H), 11.21 (br  
6 s, 1H), 7.64 (d, *J* = 8.1 Hz, 2H), 7.51 (d, *J* = 8.1 Hz, 2H), 7.30 (s, 1H), 2.05 (s, 3H) ppm. <sup>13</sup>C  
7 NMR (125 MHz, DMSO-*d*<sub>6</sub>) δ 168.5, 141.4, 137.1, 135.1, 134.3, 126.2, 109.9, 90.9, 22.8.  
8 LCMS (ESI<sup>-</sup>) *m/z* 326.0 [M - H]<sup>-</sup>, retention time 2.43 min (100%). HRMS (ESI<sup>+</sup>): *m/z*  
9 calculated for C<sub>11</sub>H<sub>11</sub>IN<sub>3</sub>O [M + H]<sup>+</sup>: 327.9947. Found: 327.9945.  
10  
11  
12  
13  
14  
15  
16  
17

18 **4-(4-bromophenyl)-1*H*-imidazol-2-amine (50)**. Following the general method G, from *N*-(4-  
19 (4-bromophenyl)-1*H*-imidazol-2-yl)acetamide **45** (88 mg, 0.31 mmol) was obtained **50** (70 mg,  
20 0.29 mmol, 95% yield) as a brown solid. <sup>1</sup>H NMR (500 MHz, DMSO-*d*<sub>6</sub>) δ 7.52 (d, *J* = 8.1 Hz,  
21 2H), 7.42 (d, *J* = 8.6 Hz, 2H), 7.04 (s, 1H), 5.40 (br s, 2H) ppm. <sup>13</sup>C NMR (126 MHz, DMSO-  
22 *d*<sub>6</sub>) δ 150.4, 134.0, 131.2, 126.0, 125.4, 117.5, 110.5 ppm. LCMS (ESI<sup>+</sup>) *m/z* 240.1 [M + H]<sup>+</sup>,  
23 retention time 1.50 min (97%). HRMS (ESI<sup>+</sup>): *m/z* calculated for C<sub>9</sub>H<sub>9</sub>BrN<sub>3</sub> [M + H]<sup>+</sup>:  
24 237.9980. Found: 237.9980. NMR data is in accordance with literature values.<sup>37</sup>  
25  
26  
27  
28  
29  
30  
31  
32  
33

34 **4-phenyl-1*H*-imidazol-2-amine (51)**. Following the general method G, from *N*-(4-phenyl-1*H*-  
35 imidazol-2-yl)acetamide **46** (70 mg, 0.35 mmol) was obtained **51** (47 mg, 0.29 mmol, 84%  
36 yield) as a red solid. <sup>1</sup>H NMR (400 MHz, MeOD) δ 7.62 – 7.46 (m, 2H), 7.31 (t, *J* = 7.7 Hz,  
37 2H), 7.16 (td, *J* = 7.5, 1.2 Hz, 1H), 6.91 (s, 1H) ppm. <sup>13</sup>C NMR (125 MHz, MeOD) δ 150.3,  
38 132.9, 128.4, 128.1, 125.6, 123.5, 111.2 ppm. LCMS (ESI<sup>+</sup>) *m/z* 160.1 [M + H]<sup>+</sup>, retention time  
39 1.45 min (100%). HRMS (ESI<sup>+</sup>): *m/z* calculated for C<sub>9</sub>H<sub>10</sub>BrN<sub>3</sub> [M + H]<sup>+</sup>: 160.0875. Found:  
40 160.0873. NMR data is in accordance with literature values.<sup>37</sup>  
41  
42  
43  
44  
45  
46  
47  
48  
49

50 **4-(4-morpholinophenyl)-1*H*-imidazol-2-amine (52)**. Following the general method G, from  
51 *N*-(4-(4-morpholinophenyl)-1*H*-imidazol-2-yl)acetamide **47** (85 mg, 0.30 mmol) was obtained  
52 **52** (60 mg, 0.24 mmol, 82% yield) as a brown solid. <sup>1</sup>H NMR (400 MHz, MeOD) δ 7.47 (d, *J* =  
53 8.8 Hz, 2H), 6.96 (d, *J* = 8.8 Hz, 2H), 6.78 (s, 1H), 3.91 – 3.64 (m, 4H), 3.19 – 3.02 (m, 4H)  
54  
55  
56  
57  
58  
59  
60

1  
2  
3 ppm.  $^{13}\text{C}$  NMR (126 MHz, MeOD)  $\delta$  149.9, 149.8, 129.3, 125.0, 124.5, 115.8, 113.0, 66.6, 49.4  
4  
5 ppm. LCMS (ESI+)  $m/z$  245.1  $[\text{M} + \text{H}]^+$ , retention time 1.50 min (100%). HRMS (ESI+):  $m/z$   
6  
7 calculated for  $\text{C}_{13}\text{H}_{17}\text{N}_4\text{O}$   $[\text{M} + \text{H}]^+$ : 245.1402. Found: 245.1390.  
8  
9

10  
11 **4-(4-methoxyphenyl)-1H-imidazol-2-amine (53)**. Following the general method G, from *N*-(4-  
12  
13 (4-methoxyphenyl)-1H-imidazol-2-yl)acetamide **48** (83 mg, 0.36 mmol) was obtained **53** (65  
14  
15 mg, 0.34 mmol, 95% yield) as a brown solid.  $^1\text{H}$  NMR (400 MHz, MeOD)  $\delta$  7.54 – 7.39 (m,  
16  
17 2H), 7.04 – 6.85 (m, 2H), 6.78 (s, 1H), 3.81 (s, 3H) ppm.  $^{13}\text{C}$  NMR (100 MHz, MeOD)  $\delta$  158.3,  
18  
19 150.0, 125.9, 125.0, 124.8, 113.6, 109.8, 54.3 ppm. LCMS (ESI+)  $m/z$  190.2  $[\text{M} + \text{H}]^+$ ,  
20  
21 retention time 1.61 min (100%). HRMS (ESI+):  $m/z$  calculated for  $\text{C}_{10}\text{H}_{12}\text{N}_3\text{O}$   $[\text{M} + \text{H}]^+$ :  
22  
23 190.0980. Found: 190.0979. NMR data is in accordance with literature values.<sup>37</sup>  
24  
25

26  
27 **4-(4-iodophenyl)-1H-imidazol-2-amine (54)**. Following the general method G, from *N*-(4-(4-  
28  
29 iodophenyl)-1H-imidazol-2-yl)acetamide **49** (150 mg, 0.46 mmol) was obtained **54** (103 mg,  
30  
31 0.36 mmol, 79% yield) as a red solid.  $^1\text{H}$  NMR (500 MHz,  $\text{DMSO-}d_6$ )  $\delta$  7.58 (d,  $J = 8.3$  Hz,  
32  
33 2H), 7.38 (d,  $J = 8.2$  Hz, 2H), 7.03 (s, 1H), 5.35 (br s, 2H) ppm.  $^{13}\text{C}$  NMR (126 MHz,  $\text{DMSO-}$   
34  
35  $d_6$ )  $\delta$  150.8, 137.4, 134.6, 133.4, 126.0, 111.1, 90.2 ppm. LCMS (ESI+)  $m/z$  286.1  $[\text{M} + \text{H}]^+$ ,  
36  
37 retention time 2.09 min (100%). HRMS (ESI+):  $m/z$  calculated for  $\text{C}_9\text{H}_9\text{IN}_3$   $[\text{M} + \text{H}]^+$ :  
38  
39 285.9841. Found: 285.9846.  
40  
41

42  
43 **4-(1H-imidazol-4-yl)phenol (55)**. 2-bromo-1-(4-hydroxyphenyl)ethan-1-one (1.0 g, 4.67  
44  
45 mmol) was dissolved in formamide (5 mL) and the reaction mixture was heated at 150°C for 24  
46  
47 h. After cooling to rt, the resulting mixture was diluted with EtOAc (40 mL) and washed with  
48  
49 saturated aqueous  $\text{NaHCO}_3$  (40 mL). The aqueous layer was extracted with EtOAc (2 x 40 mL),  
50  
51 and the combined organic layers were dried over  $\text{MgSO}_4$ , filtered, and concentrated to give **55**  
52  
53 (0.75 g, 4.67 mmol, 99% yield) as a brown oil.  $^1\text{H}$  NMR (400 MHz, MeOD)  $\delta$  8.17 (br s, 1H),  
54  
55 7.68 (d,  $J = 1.2$  Hz, 1H), 7.64 – 7.44 (m, 2H), 7.25 (d,  $J = 1.1$  Hz, 1H), 6.82 (d,  $J = 8.6$  Hz, 2H)  
56  
57 ppm.  $^{13}\text{C}$  NMR (101 MHz, MeOD)  $\delta$  156.3, 135.1, 125.8, 124.3, 115.1 ppm. LCMS (ESI+)  $m/z$   
58  
59  
60

1  
2  
3 161.2 [M + H]<sup>+</sup>, retention time 0.54 min (100%). HRMS (ESI<sup>+</sup>): m/z calculated for C<sub>9</sub>H<sub>9</sub>N<sub>2</sub>O  
4 [M + H]<sup>+</sup>: 161.0715. Found: 161.0720. NMR data is in accordance with literature values.<sup>38</sup>  
5  
6  
7

8 **4-(4-methoxyphenyl)-1-methyl-1H-imidazole (56)**. To a solution of **55** (2.77 g, 17 mmol) in  
9 DMF (20 mL) containing cesium carbonate (12.4 g, 38 mmol) at rt was added iodomethane (2.4  
10 mL, 38 mmol). The reaction mixture was stirred at rt for 8 h. The reaction mixture was then  
11 cooled to 0 °C and quenched with H<sub>2</sub>O (70 mL) and extracted with EtOAc (3 x 60 mL). The  
12 combined organic layers were washed with brine (3 x 100 mL), dried over MgSO<sub>4</sub>, filtered, and  
13 concentrated to give **56** (2.8 g, 15 mmol, 88% yield) as a brown solid. <sup>1</sup>H NMR (400 MHz,  
14 CDCl<sub>3</sub>) δ 7.71 (d, *J* = 8.8 Hz, 2H), 7.46 (d, *J* = 1.3 Hz, 1H), 7.10 (d, *J* = 1.4 Hz, 1H), 6.94 (d, *J*  
15 = 8.9 Hz, 2H), 3.85 (s, 3H), 3.73 (s, 3H) ppm. <sup>13</sup>C NMR (100 MHz, CDCl<sub>3</sub>) δ 158.6, 142.4,  
16 137.8, 127.2, 126.0, 114.8, 114.0, 55.3, 33.5. LCMS (ESI<sup>+</sup>) m/z 189.2 [M + H]<sup>+</sup>, retention time  
17 1.38 min (100%). HRMS (ESI<sup>+</sup>): m/z calculated for C<sub>11</sub>H<sub>13</sub>N<sub>2</sub>O [M + H]<sup>+</sup>: 189.1028. Found:  
18 189.1031. NMR data is in accordance with literature values.<sup>41</sup>  
19  
20  
21  
22  
23  
24  
25  
26  
27  
28  
29  
30

31  
32 **4-(1-methyl-1H-imidazol-4-yl)phenol (57)**. A solution of 4-(4-methoxyphenyl)-1-methyl-1H-  
33 imidazole **56** (1.21 g, 6.42 mmol) in anhydrous DCM (30 mL) at -78 °C was treated with BBr<sub>3</sub>  
34 (16 mL, 16.05 mmol, 1M in DCM). The reaction mixture was stirred at -78 °C for 10 min and 2  
35 h at rt. The reaction mixture was then cooled to -78 °C and quenched with MeOH (4 mL). The  
36 solvents were then removed under reduced pressure and the crude product was redissolved in  
37 EtOAc (50 mL) and washed with saturated NaHCO<sub>3</sub> solution. The aqueous phase was extracted  
38 with EtOAc (2 x 50 mL), and the combined organic fractions were dried with anhydrous  
39 MgSO<sub>4</sub>, filtered off and the solvent was removed under vacuum to give **57** (1.30 g, 6.17 mmol,  
40 96% yield) as a brown solid, which was used in the next step without further purification. <sup>1</sup>H  
41 NMR (400 MHz, MeOD) δ 8.99 – 8.80 (m, 1H), 7.77 (d, *J* = 1.6 Hz, 1H), 7.55 (d, *J* = 8.7 Hz,  
42 2H), 6.93 (d, *J* = 8.8 Hz, 2H), 3.99 (s, 3H) ppm. <sup>13</sup>C NMR (100 MHz, MeOD) δ 159.1, 135.1,  
43 134.6, 126.9, 117.3, 117.2, 115.8, 35.0 ppm. LCMS (ESI<sup>+</sup>) m/z 175.1 [M + H]<sup>+</sup>, retention time  
44  
45  
46  
47  
48  
49  
50  
51  
52  
53  
54  
55  
56  
57  
58  
59  
60

1  
2  
3 1.09 min (100%). HRMS (ESI+):  $m/z$  calculated for  $C_{10}H_{11}N_2O$   $[M + H]^+$ : 175.0871. Found:  
4 175.0870.  
5  
6  
7

8 **Methyl 2-(4-(1-methyl-1*H*-imidazol-4-yl)phenoxy)propanoate (58)**.  $Cs_2CO_3$  (3.46 g, 10.62  
9 mmol) and methyl 2-bromopropanoate (1.29 g, 6.81 mmol) were added to a solution of phenol  
10 derivative **57** (1.12 g, 5.32 mmol) in anhydrous DMF (10 mL), and the mixture was stirred at rt  
11 for 1 h and at 60 °C for 5h. After cooling to rt, the reaction was diluted with water (80 mL) and  
12 extracted EtOAc (2 x 80 mL). The combined organic layers were washed with brine (3 x 100  
13 mL), dried over  $MgSO_4$ , filtered, and concentrated. The crude product was purified by flash  
14 chromatography (0–20% v/v MeOH in DCM) to give **58** (1.30 g, 4.99 mmol, 92% yield) as an  
15 orange oil.  $^1H$  NMR (400 MHz,  $CDCl_3$ )  $\delta$  7.74 – 7.61 (m, 2H), 7.45 (d,  $J = 1.3$  Hz, 1H), 7.08 (d,  
16  $J = 1.4$  Hz, 1H), 6.96 – 6.81 (m, 2H), 4.81 (q,  $J = 6.8$  Hz, 1H), 3.77 (s, 3H), 3.71 (s, 3H), 1.64  
17 (d,  $J = 6.8$  Hz, 3H) ppm.  $^{13}C$  NMR (101 MHz,  $CDCl_3$ )  $\delta$  172.8, 156.5, 142.1, 137.8, 128.1,  
18 126.0, 115.3, 115.1, 72.7, 52.3, 33.5, 18.6 ppm. LCMS (ESI+)  $m/z$  261.3  $[M + H]^+$ , retention  
19 time 1.50 min (100%). HRMS (ESI+):  $m/z$  calculated for  $C_{14}H_{17}N_2O_3$   $[M + H]^+$ : 261.1239.  
20 Found: 261.1232.  
21  
22  
23  
24  
25  
26  
27  
28  
29  
30  
31  
32  
33  
34  
35

36 **2-(4-(1-methyl-1*H*-imidazol-4-yl)phenoxy)propanoic acid (59)**. Methyl 2-(4-(1-methyl-1*H*-  
37 imidazol-4-yl)phenoxy)propanoate **58** (0.53 g, 2.04 mmol) was dissolved in 2:1 v/v mixture of  
38 THF and  $H_2O$  (7.5 mL) and then NaOH (0.16 g, 4.08 mmol) was added. The reaction mixture  
39 was heated at 80 °C for 40 min. After the reaction mixture was allowed to cool to rt, the solvents  
40 were removed. The mixture was then diluted with  $H_2O$  (5 mL), acidified to pH 7–8 using 1N  
41 HCl. The mixture was cooled, and the resulting precipitate was collected by filtration, washed  
42 with water (2 x 3 mL) and petroleum ether (2 x 3 mL), and dried *in vacuo* to afford acid **59** (0.33  
43 g, 1.33 mmol, 65% yield) as a white solid.  $^1H$  NMR (400 MHz,  $DMSO-d_6$ )  $\delta$  7.69 – 7.55 (m,  
44 3H), 7.46 (d,  $J = 1.3$  Hz, 1H), 6.84 (d,  $J = 8.8$  Hz, 2H), 4.81 (q,  $J = 6.8$  Hz, 1H), 3.66 (s, 3H),  
45 1.49 (d,  $J = 6.7$  Hz, 3H).  $^{13}C$  NMR (100 MHz,  $DMSO-d_6$ )  $\delta$  173.3, 156.1, 140.4, 138.2, 127.8,  
46 125.4, 115.8, 114.8, 71.7, 33.1, 18.4. LCMS (ESI+)  $m/z$  247.2  $[M + H]^+$ , retention time 1.43  
47  
48  
49  
50  
51  
52  
53  
54  
55  
56  
57  
58  
59  
60

1  
2  
3 min (100%). HRMS (ESI+):  $m/z$  calculated for  $C_{13}H_{15}N_2O_3$   $[M + H]^+$ : 247.1083. Found:  
4  
5 247.1080.

6  
7  
8 **(S)-2-(4-(1-methyl-1H-imidazol-4-yl)phenoxy)propanoic acid ((S)-59)**. To a solution of **57**  
9  
10 (212 mg, 1.21 mmol) in anhydrous THF (5 mL) was added ethyl D-lactate (215 mg, 1.82  
11  
12 mmol). After the reaction mixture was cooled to 0 °C,  $PPh_3$  (478 mg, 1.82 mmol) and DEAD  
13  
14 (286  $\mu$ L, 1.82 mmol) were added, and the reaction mixture was stirred for 16 h at rt. The  
15  
16 reaction mixture was poured into ice-water (40 mL) and extracted with DCM (3 x 50 mL). The  
17  
18 combined organic layers were washed with brine, dried over anhydrous  $MgSO_4$ , filtered, and  
19  
20 concentrated. The crude product was purified by flash chromatography (0–15% v/v MeOH in  
21  
22 DCM) to give ethyl (S)-2-(4-(1-methyl-1H-imidazol-4-yl)phenoxy)propanoate as an orange  
23  
24 solid. LCMS (ESI+)  $m/z$  275.3  $[M + H]^+$ , retention time 2.06 min (94%). Ethyl (S)-2-(4-(1-  
25  
26 methyl-1H-imidazol-4-yl)phenoxy)propanoate (200 mg, 0.73 mmol) was dissolved in 2:1 v/v  
27  
28 mixture of THF and  $H_2O$  (7.5 mL) and then NaOH (58 mg, 1.46 mmol) was added. The reaction  
29  
30 mixture was stirred at rt for 3h, and the solvents were removed. The residue was dissolved in  
31  
32 EtOAc (40 mL) and then extracted with  $H_2O$  (40 mL). The aqueous layer was acidified to pH 7–  
33  
34 8 using 1N HCl. The mixture was cooled, and the resulting precipitate was collected by  
35  
36 filtration, washed with water (2 x 3 mL) and petroleum ether (2 x 3 mL), and dried *in vacuo* to  
37  
38 afford acid **(S)-59** (100 mg, 0.40 mmol, 56% yield) as a white solid.  $[\alpha]_D^{25}$   $-51.6$  ( $c$  1.0,  $CHCl_3$ ).  
39  
40 LCMS (ESI+)  $m/z$  247.2  $[M + H]^+$ , retention time 1.43 min (100%). HRMS (ESI+):  $m/z$   
41  
42 calculated for  $C_{13}H_{15}N_2O_3$   $[M + H]^+$ : 247.1083. Found: 247.1079.  
43  
44  
45

46 **4-(4-bromophenyl)oxazol-2-amine (61)**. A mixture of 2-bromo-1-(4-bromophenyl)ethanone  
47  
48 (200 mg, 0.72mmol) and urea (435 mg, 7.2 mmol) in anhydrous acetonitrile (5 mL) was heated  
49  
50 at 80 °C for 18h. The solvent was removed, and the residue was purified by flash  
51  
52 chromatography (0–10% v/v MeOH in DCM) to afford **61** (134 mg, 0.56 mmol, 78% yield) as a  
53  
54 yellow solid.  $^1H$  NMR (400 MHz, MeOD)  $\delta$  7.68 (s, 1H), 7.59 – 7.42 (m, 4H) ppm.  $^{13}C$  NMR  
55  
56 (125 MHz, MeOD)  $\delta$  163.9, 139.8, 132.7, 132.1, 128.8, 127.9, 122.1 ppm. LCMS (ESI+)  $m/z$   
57  
58  
59  
60

1  
2  
3 238.8 [M + H]<sup>+</sup>, retention time 1.95 min (100%). HRMS (ESI<sup>+</sup>): m/z calculated for C<sub>9</sub>H<sub>8</sub>BrN<sub>2</sub>O  
4 [M + H]<sup>+</sup>: 238.9820. Found: 238.9816.  
5  
6  
7

## 8 **2. Enzyme Assay**

9  
10 The activity of *Mth* IMPDH ΔCBS was determined using a plate reader by monitoring the  
11 production of NADH in absorbance at 340 nm and corrected for non-catalyzed chemical  
12 reactions in the absence of *Mth* IMPDH ΔCBS. All the measurements were done in the assay  
13 buffer (50 mM Tris HCl pH 8, 1 mM DTT, 1 mM EDTA and 100 mM KCl) at 37 °C with 20  
14 nM *Mth* IMPDH ΔCBS, 2.8 mM NAD<sup>+</sup> and 1 mM IMP in a total of 150 μL volume in a 96 well  
15 plate-based format and data were collected for 32 min. The reaction was initiated by the  
16 addition of the substrate, IMP, at a concentration of 1 mM. All reactions were performed in  
17 triplicates. Prior to reaction initiation, the compounds were pre-incubated in a buffer with  
18 enzyme for 5 minutes. The inhibitors were dissolved in DMSO-*d*<sub>6</sub> and diluted to a final  
19 concentration of 1% v/v in experimental reactions.  
20  
21

22 IC<sub>50</sub> values were calculated by plotting the percentage of inhibition against the logarithm of  
23 inhibitor concentration and dose-response curves were fitted using Prism software (GraphPad).  
24

25 The *K<sub>i</sub>* value for NAD<sup>+</sup> was determined at a constant saturating IMP concentration (1 mM) and  
26 five different concentrations of NAD<sup>+</sup> (0.35, 0.70, 1.0, 1.4 and 2.8 mM) in the presence of  
27 increasing concentrations of inhibitor. The value of *K<sub>i</sub>* for IMP was determined at fixed  
28 saturating concentration of NAD<sup>+</sup> (2.8 mM) and different concentrations of IMP (0.12, 0.18,  
29 0.25, 0.5 and 1 mM) and inhibitor.  
30

31 The initial velocities at various inhibitor concentrations were determined based on the slope in  
32 the linear part of each reaction containing the inhibitor and the uninhibited reaction. To  
33 determine the inhibition constant (*K<sub>i</sub>* values) the initial rate data versus substrate concentration  
34 at different inhibitor concentrations were fit using Prism software (GraphPad) to equations for  
35 uncompetitive or mixed inhibition. For each inhibitor concentration, the reciprocal of enzyme  
36 reaction velocity versus the reciprocal of the substrate concentration was plotted in a  
37 Lineweaver-Burk plot to determine the pattern of inhibition.  
38  
39  
40  
41  
42  
43  
44  
45  
46  
47  
48  
49  
50  
51  
52  
53  
54  
55  
56  
57  
58  
59  
60

### 3. Protein Purification, Crystallization and Data Collection of *Mth* IMPDH $\Delta$ CBS

*Mth* IMPDH was expressed, purified and crystallized as previously described.<sup>24, 25</sup> Briefly, hexahistidine tagged *Mth* IMPDH  $\Delta$ CBS in pHat2 was expressed overnight in BL21 DE3 (NEB) cells at 18°C by addition of 500  $\mu$ M IPTG. Cells were lysed in 50 mM Hepes, pH 8.0, 500 mM NaCl, 5% glycerol, 10 mM  $\beta$ -mercaptoethanol, and 20 mM imidazole, and the recombinant protein purified using a Hi-Trap IMAC FF column (GE Healthcare) charged with nickel and an elution gradient of up to 300 mM imidazole. The hexahistidine tag was cleaved by TEV protease, and the purified *Mth* IMPDH  $\Delta$ CBS obtained by negative nickel gravity-flow purification<sup>42</sup> and size exclusion chromatography on a Superdex 200 gel filtration column equilibrated in 20 mM Hepes pH 8.0, 500 mM NaCl, 5% glycerol, and 1 mM TCEP step. The recombinant *Mth* IMPDH  $\Delta$ CBS was then concentrated to 12.5 mg/mL for crystallization.

*Mth* IMPDH  $\Delta$ CBS protein crystallized in 1  $\mu$ L + 1  $\mu$ L hanging drops with 100 mM sodium acetate, pH 5.5, 200 mM calcium chloride, and 8–14% isopropanol. Crystals were soaked overnight in drops of well solution + 5 mM IMP and either 5 mM Fragment **2** or Compound **1** or 1 mM Compound **31**. Crystals were cryoprotected by passing through drops containing well solution + 25% glycerol and flash-frozen in liquid nitrogen. Data were collected from the crystals at Diamond Light Source beamline.

### 4. Structure Solution, Ligand Fitting, and Refinement

Data were processed using XDS<sup>43</sup> and Pointless (CCP4). To solve the structure, molecular replacement was performed with Phenix Phaser<sup>44</sup> using a previously solved IMP-bound *Mth* IMPDH  $\Delta$ CBS structure as a probe (PDB ID's: 5J5R; 5K4X; 5K4Z). Refinement was performed using Phenix.refine and manually in Coot.<sup>45</sup> IMP and the inhibitors were sequentially fitted into the density using the LigandFit function of Phenix, and the structures were manually refined further using Coot. Information regarding the crystallographic statistics can be found in Table S2. Protein–ligand interactions were analyzed using Arpeggio<sup>46</sup> and CSM-Lig.<sup>47, 48</sup> Compound properties were evaluated using pkCSM.<sup>49</sup> All figures made using Pymol (Schrodinger).

## 5. Drug susceptibility testing against *Mtb*.

An Alamar Blue fluorescence-based broth microdilution assay was used to assess minimum inhibitory concentration (MIC) of compounds against *Mtb* H37Rv, as described previously.<sup>25,50</sup> Briefly, *Mtb* H37Rv was grown in standard Middlebrook 7H9 broth (BD) supplemented with OADC (BD), 0.2% glycerol and 0.05% Tween-80 to mid-exponential phase. Compounds dissolved in DMSO (1%) were tested in clear-bottomed, round-well 96-well microtiter plates at 8 different concentrations using the standard anti-TB drugs, rifampin and isoniazid, as positive controls. An inoculum of  $\sim 10^5$  bacteria was added to each well, and the plates were incubated at 37°C for 7 d. On day 7, 10  $\mu$ L of Alamar Blue (Invitrogen) was added to each well, and plates were further incubated at 37°C for 24 h. The fluorescence (excitation 544 nm; emission 590 nm) was measured in a FLUOstar OPTIMA plate reader (BMG LABTECH, Offenberg, Germany). Data were normalized to the minimum and maximum inhibition controls to generate a dose response curve (% inhibition) from which the MIC<sub>90</sub> was determined.

## AUTHOR INFORMATION

### Corresponding Authors

D.B.A: phone, +61 3903 54794; e-mail, david.ascher@unimelb.edu.au.

C.A.: phone, +44 (0) 1223 336405; e-mail, ca26@cam.ac.uk

T.L.B. email: tom@cryst.bioc.cam.ac.uk.

## ACKNOWLEDGMENTS

This work was supported by the Bill and Melinda Gates Foundation (Hit-TB) and FP7 European Project MM4TB Grant no. 260872. D.B.A was supported by a C. J. Martin Research Fellowship from the National Health and Medical Research Council of Australia (APP1072476) and the Jack Brockhoff Foundation (JBF 4186, 2016). D.B.A. and T.L.B. were also funded by a Newton Fund RCUK-CONFAP Grant awarded by The Medical Research Council and Fundação de Amparo à Pesquisa do Estado de Minas Gerais (MR/M026302/1). V.M. and V.S. were also

1  
2  
3 supported by grants from the HHMI (Senior International Research Scholars grant to V.M.), the  
4 South African Medical Research Council and the National Research Foundation.  
5  
6  
7

## 8 **ABBREVIATIONS USED**

9  
10 TB, Tuberculosis; *Mycobacterium tuberculosis*, *Mtb*; MDR, multidrug resistant; XDR,  
11 extensively drug resistant; IMPDH, Inosine-5'-monophosphate dehydrogenase; IMP, inosine 5'-  
12 monophosphate; CBS, cystathionine  $\beta$ -synthase; XMP, xanthosine monophosphate; NAD<sup>+</sup>,  
13 nicotinamide adenine dinucleotide; *Mth*, *Mycobacterium thermoresistibile*; MIC, minimal  
14 inhibitory concentration.  
15  
16  
17  
18  
19  
20  
21

## 22 **ASSOCIATED CONTENT**

### 23 **Supporting Information**

24  
25 This material is available free of charge on the ACS Publications website.  
26  
27

28 <sup>1</sup>H, <sup>13</sup>C, and 2D NMR spectra of all new compounds, supplementary Figures S1-S2, whole-cell  
29 activity of compounds against *M. tuberculosis* H37Rv (Table S1), and X-ray data collection and  
30 refinement statistics (Table S2) (PDF).  
31  
32  
33

34 The molecular formula strings data file for all chemical structures mentioned in the manuscript  
35 is also provided (CSV).  
36  
37

38 Additional data related to this publication is available at the University of Cambridge data  
39 repository: <https://doi.org/10.17863/CAM.20512>  
40  
41  
42  
43

### 44 **Accession Codes**

45 Structures have been deposited in the Protein Data Bank (PDB codes 5OU1 for  
46 IMPDH:IMP:Compound **1**; 5OU2 for IMPDH:IMP:Compound **2** and 5OU3 for  
47 IMPDH:IMP:Compound **31** complex structures). Authors will release the atomic  
48 coordinates and experimental data upon article publication  
49  
50  
51  
52  
53

## 54 **REFERENCES**

- 1  
2  
3 (1) WHO. Tuberculosis: Fact sheet. Geneva, Switzerland: World Health Organization 2016.  
4  
5 **2016.**
- 6  
7 (2) Onyebujoh, P.; Zumla, A.; Ribeiro, I.; Rustomjee, R.; Mwaba, P.; Gomes, M.; Grange, J. M.  
8  
9 Treatment of tuberculosis: present status and future prospects. *Bull. World Health Organ.* **2005,**  
10  
11 *83*, 857-865.
- 12  
13 (3) Orenstein, E. W.; Basu, S.; Shah, N. S.; Andrews, J. R.; Friedland, G. H.; Moll, A. P.;  
14  
15 Gandhi, N. R.; Galvani, A. P. Treatment outcomes among patients with multidrug-resistant  
16  
17 tuberculosis: systematic review and meta-analysis. *Lancet Infect. Dis.* **2009**, *9*, 153-161.
- 18  
19 (4) Ratcliffe, A. J. Inosine 5'-monophosphate dehydrogenase inhibitors for the treatment of  
20  
21 autoimmune diseases. *Curr. Opin. Drug Discov. Devel.* **2006**, *9*, 595-605.
- 22  
23 (5) Chen, L.; Pankiewicz, K. W. Recent development of IMP dehydrogenase inhibitors for the  
24  
25 treatment of cancer. *Curr. Opin. Drug Discov. Devel.* **2007**, *10*, 403-412.
- 26  
27 (6) Olah, E.; Kokeny, S.; Papp, J.; Bozsik, A.; Keszei, M. Modulation of cancer pathways by  
28  
29 inhibitors of guanylate metabolism. *Adv. Enzyme Regul.* **2006**, *46*, 176-190.
- 30  
31 (7) Nair, V.; Shu, Q. Inosine monophosphate dehydrogenase as a probe in antiviral drug  
32  
33 discovery. *Antivir. Chem. Chemother.* **2007**, *18*, 245-258.
- 34  
35 (8) Shu, Q.; Nair, V. Inosine monophosphate dehydrogenase (IMPDH) as a target in drug  
36  
37 discovery. *Med. Res. Rev.* **2008**, *28*, 219-232.
- 38  
39 (9) Shah, C. P.; Kharkar, P. S. Inosine 5'-monophosphate dehydrogenase inhibitors as  
40  
41 antimicrobial agents: recent progress and future perspectives. *Future Med. Chem.* **2015**, *7*,  
42  
43 1415-1429.
- 44  
45 (10) Hedstrom, L.; Liechti, G.; Goldberg, J. B.; Gollapalli, D. R. The antibiotic potential of  
46  
47 prokaryotic IMP dehydrogenase inhibitors. *Curr. Med. Chem.* **2011**, *18*, 1909-1918.
- 48  
49 (11) Hedstrom, L. IMP dehydrogenase: structure, mechanism, and inhibition. *Chem. Rev.* **2009**,  
50  
51 *109*, 2903-2928.
- 52  
53 (12) Jackson, R. C.; Weber, G.; Morris, H. P. IMP dehydrogenase, an enzyme linked with  
54  
55 proliferation and malignancy. *Nature* **1975**, *256*, 331-333.
- 56  
57  
58  
59  
60

- 1  
2  
3 (13) Gilbert, H. J.; Lowe, C. R.; Drabble, W. T. Inosine 5'-monophosphate dehydrogenase of  
4 Escherichia coli. Purification by affinity chromatography, subunit structure and inhibition by  
5 guanosine 5'-monophosphate. *Biochem. J.* **1979**, *183*, 481-494.  
6  
7  
8 (14) Lee, S. A.; Gallagher, L. A.; Thongdee, M.; Staudinger, B. J.; Lippman, S.; Singh, P. K.;  
9 Manoil, C. General and condition-specific essential functions of *Pseudomonas aeruginosa*.  
10 *Proc. Natl. Acad. Sci. U S A* **2015**, *112*, 5189-5194.  
11  
12  
13 (15) Valentino, M. D.; Foulston, L.; Sadaka, A.; Kos, V. N.; Villet, R. A.; Santa Maria, J., Jr.;  
14 Lazinski, D. W.; Camilli, A.; Walker, S.; Hooper, D. C.; Gilmore, M. S. Genes contributing to  
15 *Staphylococcus aureus* fitness in abscess- and infection-related ecologies. *MBio* **2014**, *5*,  
16 e01729-14.  
17  
18  
19 (16) Sassetti, C. M.; Boyd, D. H.; Rubin, E. J. Genes required for mycobacterial growth defined  
20 by high density mutagenesis. *Mol. Microbiol.* **2003**, *48*, 77-84.  
21  
22  
23 (17) Hedstrom, L. The bare essentials of antibiotic target validation. *ACS Infect. Dis.* **2017**, *3*, 2-  
24 4.  
25  
26  
27 (18) Petrelli, R.; Vita, P.; Torquati, I.; Felczak, K.; Wilson, D. J.; Franchetti, P.; Cappellacci, L.  
28 Novel inhibitors of inosine monophosphate dehydrogenase in patent literature of the last decade.  
29 *Recent Pat. Anticancer Drug Discov.* **2013**, *8*, 103-125.  
30  
31  
32 (19) Makowska-Grzyska, M.; Kim, Y.; Wu, R.; Wilton, R.; Gollapalli, D. R.; Wang, X. K.;  
33 Zhang, R.; Jedrzejczak, R.; Mack, J. C.; Maltseva, N.; Mulligan, R.; Binkowski, T. A.;  
34 Gornicki, P.; Kuhn, M. L.; Anderson, W. F.; Hedstrom, L.; Joachimiak, A. *Bacillus anthracis*  
35 inosine 5'-monophosphate dehydrogenase in action: the first bacterial series of structures of  
36 phosphate ion-, substrate-, and product-bound complexes. *Biochemistry* **2012**, *51*, 6148-6163.  
37  
38  
39 (20) Usha, V.; Gurucha, S. S.; Lovering, A. L.; Lloyd, A. J.; Papaemmanouil, A.; Reynolds, R.  
40 C.; Besra, G. S. Identification of novel diphenyl urea inhibitors of Mt-GuaB2 active against  
41 *Mycobacterium tuberculosis*. *Microbiology* **2011**, *157*, 290-299.  
42  
43  
44 (21) Makowska-Grzyska, M.; Kim, Y.; Gorla, S. K.; Wei, Y.; Mandapati, K.; Zhang, M.;  
45 Maltseva, N.; Modi, G.; Boshoff, H. I.; Gu, M.; Aldrich, C.; Cuny, G. D.; Hedstrom, L.;  
46  
47  
48  
49  
50  
51  
52  
53  
54  
55  
56  
57  
58  
59  
60

1  
2  
3 Joachimiak, A. *Mycobacterium tuberculosis* IMPDH in complexes with substrates, products and  
4 antitubercular compounds. *PLoS One* **2015**, *10*, e0138976.

5  
6 (22) Chen, L.; Wilson, D. J.; Xu, Y.; Aldrich, C. C.; Felczak, K.; Sham, Y. Y.; Pankiewicz, K.  
7  
8 W. Triazole-linked inhibitors of inosine monophosphate dehydrogenase from human and  
9  
10 *Mycobacterium tuberculosis*. *J. Med. Chem.* **2010**, *53*, 4768-4778.

11  
12 (23) Usha, V.; Hobrath, J. V.; Gurcha, S. S.; Reynolds, R. C.; Besra, G. S. Identification of  
13  
14 novel Mt-Guab2 inhibitor series active against *M. tuberculosis*. *PLoS One* **2012**, *7*, e33886.

15  
16 (24) Park, Y.; Pacitto, A.; Bayliss, T.; Cleghorn, L. A.; Wang, Z.; Hartman, T.; Arora, K.;  
17  
18 Ioerger, T. R.; Sacchettini, J.; Rizzi, M.; Donini, S.; Blundell, T. L.; Ascher, D. B.; Rhee, K. Y.;  
19  
20 Breda, A.; Zhou, N.; Dartois, V.; Jonnala, S. R.; Via, L. E.; Mizrahi, V.; Epemolu, O.;  
21  
22 Stojanovski, L.; Simeons, F. R.; Osuna-Cabello, M.; Ellis, L.; MacKenzie, C. J.; Smith, A. R.;  
23  
24 Davis, S. H.; Murugesan, D.; Buchanan, K. I.; Turner, P. A.; Huggett, M.; Zuccotto, F.;  
25  
26 Rebollo-Lopez, M. J.; Lafuente-Monasterio, M. J.; Sanz, O.; Santos Diaz, G.; Lelievre, J.;  
27  
28 Ballell, L.; Selenski, C.; Axtman, M.; Ghidelli-Disse, S.; Pflaumer, H.; Boesche, M.; Drewes,  
29  
30 G.; Freiberg, G.; Kurnick, M. D.; Srikumaran, M.; Kempf, D. J.; Green, S. R.; Ray, P. C.; Read,  
31  
32 K. D.; Wyatt, P. G.; Barry Rd, C. E.; Boshoff, H. I. Essential but not vulnerable: indazole  
33  
34 sulfonamides targeting inosine monophosphate dehydrogenase as potential leads against  
35  
36 *Mycobacterium tuberculosis*. *ACS Infect. Dis.* **2017**, *3*, 18-23.

37  
38 (25) Singh, V.; Donini, S.; Pacitto, A.; Sala, C.; Hartkoorn, R. C.; Dhar, N.; Keri, G.; Ascher, D.  
39  
40 B.; Mondesert, G.; Vocat, A.; Lupien, A.; Sommer, R.; Vermet, H.; Lagrange, S.; Buechler, J.;  
41  
42 Warner, D. F.; McKinney, J. D.; Pato, J.; Cole, S. T.; Blundell, T. L.; Rizzi, M.; Mizrahi, V.  
43  
44 The inosine monophosphate dehydrogenase, Guab2, is a vulnerable new bactericidal drug target  
45  
46 for tuberculosis. *ACS Infect. Dis.* **2017**, *3*, 5-17.

47  
48 (26) Cox, J. A.; Mugumbate, G.; Del Peral, L. V.; Jankute, M.; Abrahams, K. A.; Jervis, P.;  
49  
50 Jackenkroll, S.; Perez, A.; Alemparte, C.; Esquivias, J.; Lelievre, J.; Ramon, F.; Barros, D.;  
51  
52 Ballell, L.; Besra, G. S. Novel inhibitors of *Mycobacterium tuberculosis* Guab2 identified by a  
53  
54 target based high-throughput phenotypic screen. *Sci. Rep.* **2016**, *6*, 38986.

- 1  
2  
3 (27) Moffat, J. G.; Vincent, F.; Lee, J. A.; Eder, J.; Prunotto, M. Opportunities and challenges in  
4 phenotypic drug discovery: an industry perspective. *Nat. Rev. Drug Discov.* **2017**, *16*, 531-543.  
5  
6 (28) Koul, A.; Arnoult, E.; Lounis, N.; Guillemont, J.; Andries, K. The challenge of new drug  
7 discovery for tuberculosis. *Nature* **2011**, *469*, 483-490.  
8  
9 (29) Payne, D. J.; Gwynn, M. N.; Holmes, D. J.; Pompliano, D. L. Drugs for bad bugs:  
10 confronting the challenges of antibacterial discovery. *Nat. Rev. Drug Discov.* **2007**, *6*, 29-40.  
11  
12 (30) Scott, D. E.; Coyne, A. G.; Hudson, S. A.; Abell, C. Fragment-based approaches in drug  
13 discovery and chemical biology. *Biochemistry* **2012**, *51*, 4990-5003.  
14  
15 (31) Mendes, V.; Blundell, T. L. Targeting tuberculosis using structure-guided fragment-based  
16 drug design. *Drug Discov. Today* **2017**, *22*, 546-554.  
17  
18 (32) Marchetti, C.; Chan, D. S.; Coyne, A. G.; Abell, C. Fragment-based approaches to TB  
19 drugs. *Parasitology* **2016**, 1-12.  
20  
21 (33) Wei, Y.; Kuzmic, P.; Yu, R.; Modi, G.; Hedstrom, L. Inhibition of inosine-5'-  
22 monophosphate dehydrogenase from *Bacillus anthracis*: Mechanism revealed by pre-steady-  
23 state kinetics. *Biochemistry* **2016**, *55*, 5279-5288.  
24  
25 (34) Dunkern, T.; Prabhu, A.; Kharkar, P. S.; Goebel, H.; Rolser, E.; Burckhard-Boer, W.;  
26 Arumugam, P.; Makhija, M. T. Virtual and experimental high-throughput screening (HTS) in  
27 search of novel inosine 5'-monophosphate dehydrogenase II (IMPDH II) inhibitors. *J. Comput.*  
28 *Aided Mol. Des.* **2012**, *26*, 1277-1292.  
29  
30 (35) Gorla, S. K.; Kavitha, M.; Zhang, M.; Chin, J. E.; Liu, X.; Striepen, B.; Makowska-  
31 Grzyska, M.; Kim, Y.; Joachimiak, A.; Hedstrom, L.; Cuny, G. D. Optimization of  
32 benzoxazole-based inhibitors of *Cryptosporidium parvum* inosine 5'-monophosphate  
33 dehydrogenase. *J. Med. Chem.* **2013**, *56*, 4028-4043.  
34  
35 (36) Kitagawa, H.; Ozawa, T.; Takahata, S.; Iida, M.; Saito, J.; Yamada, M. Phenylimidazole  
36 derivatives of 4-pyridone as dual inhibitors of bacterial enoyl-acyl carrier protein reductases  
37 FabI and FabK. *J. Med. Chem.* **2007**, *50*, 4710-4720.  
38  
39 (37) Soh, C. H.; Chui, W. K.; Lam, Y. An efficient and expeditious synthesis of di- and  
40 monosubstituted 2-aminoimidazoles. *J. Comb. Chem.* **2008**, *10*, 118-122.  
41  
42  
43  
44  
45  
46  
47  
48  
49  
50  
51  
52  
53  
54  
55  
56  
57  
58  
59  
60

- 1  
2  
3 (38) Kumar, S.; Jaller, D.; Patel, B.; LaLonde, J. M.; DuHadaway, J. B.; Malachowski, W. P.;  
4 Prendergast, G. C.; Muller, A. J. Structure based development of phenylimidazole-derived  
5 inhibitors of indoleamine 2,3-dioxygenase. *J. Med. Chem.* **2008**, *51*, 4968-4977.  
6  
7  
8 (39) Jost, C.; Nitsche, C.; Scholz, T.; Roux, L.; Klein, C. D. Promiscuity and selectivity in  
9 covalent enzyme inhibition: a systematic study of electrophilic fragments. *J. Med. Chem.* **2014**,  
10 *57*, 7590-7599.  
11  
12  
13 (40) Fortin, S.; Moreau, E.; Lacroix, J.; Cote, M. F.; Petitclerc, E.; R, C. G. Synthesis,  
14 antiproliferative activity evaluation and structure-activity relationships of novel aromatic urea  
15 and amide analogues of N-phenyl-N'-(2-chloroethyl)ureas. *Eur. J. Med. Chem.* **2010**, *45*, 2928-  
16 2937.  
17  
18 (41) Bellina, F.; Guazzelli, N.; Lessi, M.; Manzini, C. Imidazole analogues of resveratrol:  
19 synthesis and cancer cell growth evaluation. *Tetrahedron* **2015**, *71*, 2298-2305.  
20  
21  
22 (42) Ascher, D. B.; Cromer, B. A.; Morton, C. J.; Volitakis, I.; Cherny, R. A.; Albiston, A. L.;  
23 Chai, S. Y.; Parker, M. W. Regulation of insulin-regulated membrane aminopeptidase activity  
24 by its C-terminal domain. *Biochemistry* **2011**, *50*, 2611-2622.  
25  
26  
27 (43) Kabsch, W. Xds. *Acta Crystallogr. D Biol. Crystallogr.* **2010**, *66*, 125-132.  
28  
29 (44) Adams, P. D.; Afonine, P. V.; Bunkoczi, G.; Chen, V. B.; Davis, I. W.; Echols, N.; Headd,  
30 J. J.; Hung, L. W.; Kapral, G. J.; Grosse-Kunstleve, R. W.; McCoy, A. J.; Moriarty, N. W.;  
31 Oeffner, R.; Read, R. J.; Richardson, D. C.; Richardson, J. S.; Terwilliger, T. C.; Zwart, P. H.  
32 PHENIX: a comprehensive Python-based system for macromolecular structure solution. *Acta*  
33 *Crystallogr. D Biol. Crystallogr.* **2010**, *66*, 213-221.  
34  
35 (45) Emsley, P.; Cowtan, K. Coot: model-building tools for molecular graphics. *Acta*  
36 *Crystallogr. D Biol. Crystallogr.* **2004**, *60*, 2126-2132.  
37  
38 (46) Jubb, H. C.; Higuieruelo, A. P.; Ochoa-Montano, B.; Pitt, W. R.; Ascher, D. B.; Blundell, T.  
39 L. Arpeggio: A web server for calculating and visualising interatomic interactions in protein  
40 structures. *J. Mol. Biol.* **2017**, *429*, 365-371.  
41  
42  
43  
44  
45  
46  
47  
48  
49  
50  
51  
52  
53  
54  
55  
56  
57  
58  
59  
60

1  
2  
3 (47) Pires, D. E.; Blundell, T. L.; Ascher, D. B. mCSM-lig: quantifying the effects of mutations  
4 on protein-small molecule affinity in genetic disease and emergence of drug resistance. *Sci. Rep.*  
5 **2016**, *6*, 29575.  
6  
7

8 (48) Pires, D. E.; Ascher, D. B. CSM-lig: a web server for assessing and comparing protein-  
9 small molecule affinities. *Nucleic Acids Res.* **2016**, *44*, W557-61.  
10  
11

12 (49) Pires, D. E.; Blundell, T. L.; Ascher, D. B. pkCSM: Predicting small-molecule  
13 pharmacokinetic and toxicity properties using graph-based signatures. *J. Med. Chem.* **2015**, *58*,  
14 4066-4072.  
15  
16  
17

18 (50) Singh, V.; Brecik, M.; Mukherjee, R.; Evans, J. C.; Svetlikova, Z.; Blasko, J.; Surade, S.;  
19 Blackburn, J.; Warner, D. F.; Mikusova, K.; Mizrahi, V. The complex mechanism of  
20 antimycobacterial action of 5-fluorouracil. *Chem. Biol.* **2015**, *22*, 63-75.  
21  
22  
23  
24  
25  
26  
27  
28  
29  
30  
31  
32  
33  
34  
35  
36  
37  
38  
39  
40  
41  
42  
43  
44  
45  
46  
47  
48  
49  
50  
51  
52  
53  
54  
55  
56  
57  
58  
59  
60

## Table of Contents Graphic

